



**HAL**  
open science

# Surface heat flow, crustal temperatures and mantle heat flow in the Proterozoic Trans-Hudson Orogen, Canadian Shield

F. Rolandone, C. Jaupart, J. C. Mareschal, C. Gariépy, G. Bienfait, C. Carbonne, R. Lapointe

## ► To cite this version:

F. Rolandone, C. Jaupart, J. C. Mareschal, C. Gariépy, G. Bienfait, et al.. Surface heat flow, crustal temperatures and mantle heat flow in the Proterozoic Trans-Hudson Orogen, Canadian Shield. *Journal of Geophysical Research: Solid Earth*, 2022, 107, 10.1029/2001JB000698 . insu-03597782

**HAL Id: insu-03597782**

**<https://insu.hal.science/insu-03597782>**

Submitted on 4 Mar 2022

**HAL** is a multi-disciplinary open access archive for the deposit and dissemination of scientific research documents, whether they are published or not. The documents may come from teaching and research institutions in France or abroad, or from public or private research centers.

L'archive ouverte pluridisciplinaire **HAL**, est destinée au dépôt et à la diffusion de documents scientifiques de niveau recherche, publiés ou non, émanant des établissements d'enseignement et de recherche français ou étrangers, des laboratoires publics ou privés.

Copyright

## Surface heat flow, crustal temperatures and mantle heat flow in the Proterozoic Trans-Hudson Orogen, Canadian Shield

F. Rolandone,<sup>1</sup> C. Jaupart,<sup>1</sup> J. C. Mareschal,<sup>2</sup> C. Gariépy,<sup>2</sup> G. Bienfait,<sup>1</sup> C. Carbonne,<sup>1</sup> and R. Lapointe<sup>2</sup>

Received 4 July 2001; revised 10 April 2002; accepted 15 April 2002; published 12 December 2002.

[1] The Paleo-Proterozoic (1.8 Ga) Trans-Hudson Orogen (THO), of intermediate age between the Superior (2.7 Ga) and Grenville (1.0 Ga) provinces, is located near the center of the Canadian Shield. We report on new measurements of heat flow and radiogenic heat production in 30 boreholes at 17 locations in this province. With these data, reliable values of heat flow and heat production are available at 45 sites in the THO. The mean and standard deviation of heat flow values are  $42 \pm 9 \text{ mW m}^{-2}$ . In this province, distinctive geological domains are associated with specific heat flow distributions. The heat flow pattern follows the surface geology with a central area of low values over an ancient back arc basin (Kisseynew) and an ancient island arc (Lynn Lake Belt) made of depleted juvenile rocks. Higher heat flow values found in peripheral belts are associated with recycled Archean crust. Within the Canadian Shield, there is no significant variation in heat flow as a function of age between provinces spanning about 2 Gyr. There is no geographic trend in heat flow across the Canadian Shield from the THO to the Labrador Sea. Low heat flow areas where the crustal structure is well-known are used to determine an upper bound of  $16 \text{ mW m}^{-2}$  for the mantle heat flow. Present and paleogeotherms are calculated for a high heat flow area in the Thompson metasedimentary belt. The condition that melting temperatures were not reached in Proterozoic times yields a lower bound of  $11\text{--}12 \text{ mW m}^{-2}$  for the mantle heat flow. **INDEX TERMS:** 8130 Tectonophysics: Evolution of the Earth: Heat generation and transport; 8120 Tectonophysics: Dynamics of lithosphere and mantle—general; 1020 Geochemistry: Composition of the crust; 8015 Structural Geology: Local crustal structure; **KEYWORDS:** heat flow measurements, crustal thermal structure, mantle heat flow

**Citation:** Rolandone, F., C. Jaupart, J. C. Mareschal, C. Gariépy, G. Bienfait, C. Carbonne, and R. Lapointe, Surface heat flow, crustal temperatures and mantle heat flow in the Proterozoic Trans-Hudson Orogen, Canadian Shield, *J. Geophys. Res.*, 107(B12), 2341, doi:10.1029/2001JB000698, 2002.

### 1. Introduction

[2] The thermal structures of continental crust and lithosphere remain poorly constrained because the crustal heat production and the mantle heat flow are not precisely known. It has generally been assumed that one may separate a deep thermal signal from crustal noise by defining global trends in heat flow. One such trend is the relationship between heat flow and age, which may be interpreted in two different ways. It may show the return to secular thermal equilibrium after a major thermal/tectonic perturbation or an intrinsic difference of lithosphere thickness between cratons and younger belts

[Nyblade and Pollack, 1993]. Both interpretations rely on the assumption that crustal heat production does not vary with age, which is not true [Morgan, 1985; Rudnick and Fountain, 1995]. Thus one must evaluate simultaneously surface heat flow and crustal heat generation in the same geological province, which requires detailed multidisciplinary surveys.

[3] In the Canadian Shield, the Paleo-Proterozoic (1.8 Ga) Trans-Hudson Orogen (THO) welds together three Archean cratons, the Superior Province to the east, the Rea-Hearne to the west and the smaller Sask craton to the south. The THO is of special interest for heat flow studies because it is of intermediate age between the well-sampled Superior (2.7 Ga) and Grenville (1.0 Ga) provinces and because it is located almost at the center of the North American continent. Therefore it provides key data for assessing thermal models for the continental lithosphere. Another reason for studying the THO is that, over relatively small distances, it brings together several distinctive belts of different origin, structure and composition. This province

<sup>1</sup>Laboratoire de Dynamique des Systèmes Géologiques, Institut de Physique du Globe de Paris, Paris, France.

<sup>2</sup>GEOTOP, Centre de Recherche en Géochimie et en Géodynamique, Université du Québec à Montréal, Montréal, Québec, Canada.

thus allows clear documentation of heat flow changes due to variations of crustal heat production.

[4] Previous work in the THO has shown that its heat flow field is extremely variable, with the highest and lowest values of the entire Canadian Shield [Drury, 1985; Guillou-Frottier *et al.*, 1996; Mareschal *et al.*, 1999a]. The data available until now were scattered over the whole province and we have gone back to the THO with two goals. One was to further our sampling of several key areas which remained poorly documented. The other goal was to investigate the length scales of heat flow variations in order to determine reliable averages for the major belts of the THO. In this paper, we report on 17 additional heat flow measurements in the THO obtained from temperature and conductivity logs in 30 individual boreholes. The U, Th and K concentrations of the main rock types were also determined systematically. These new data raise the number of heat flow values available in the THO to 45. We discuss briefly the constraints brought by heat flow data on crustal structure and lower crustal composition. We then evaluate the THO heat flow in the larger context of the whole North American craton. Low heat flow areas where the local crustal structure is well-known are used to determine an upper bound for the mantle heat flow. Next, we use a high heat flow area and derive crustal geotherms at the time the THO stabilized. We suggest that the condition that melting temperatures were not reached leads to a lower bound for the mantle heat flow.

## 2. Trans-Hudson Orogen

[5] The THO is exposed only in northern Manitoba and Saskatchewan, and can be followed by geophysical anomalies under the Paleozoic sediments of the Williston and Hudson Bay basins to the south and to the north respectively. In the exposed part of the THO, the volume of juvenile crust suggests that large amounts of new crustal material were extracted from the mantle during the Paleoproterozoic. Four major tectonic zones have been identified in the THO [Lucas *et al.*, 1993; Lewry *et al.*, 1994]: (1) The Churchill-Superior boundary, a narrow zone, along the margin of the Superior craton, including the Thompson belt, (2) the central Reindeer tectonic zone, a ~400 km wide zone including several belts of arc volcanics and metasediments, (3) the Wathaman batholith, an Andean-type magmatic arc, and (4) a deformed "hinterland" including the Wollaston fold belt. Juvenile Proterozoic crust is found in the Reindeer tectonic zone which contains several distinctive belts (Figure 1): (1) the Lynn Lake and La Ronge belts to the northwest that are formed of island arc volcanic rocks, (2) the Kisseynew domain and the McLean belt, made up of gneisses and interpreted as metasediments of a back arc basin, (3) the Glennie domain that contains metavolcanics, and (4) the Flin Flon and Snow Lake Belts made up of arc volcanic and plutonic rocks.

[6] The different units of the THO were brought together by the closure of a marginal or small ocean basin whose remnant lies beneath the Kisseynew Domain. The Rae-Hearne and Superior cratons bound the orogen to the east and the west; recent studies have revealed the smaller Sask craton to the south [Lucas *et al.*, 1993; Ashton *et al.*, 1999]. For the sake of simplicity, we divide the THO into four units with rocks of different origins and tectonic histories and

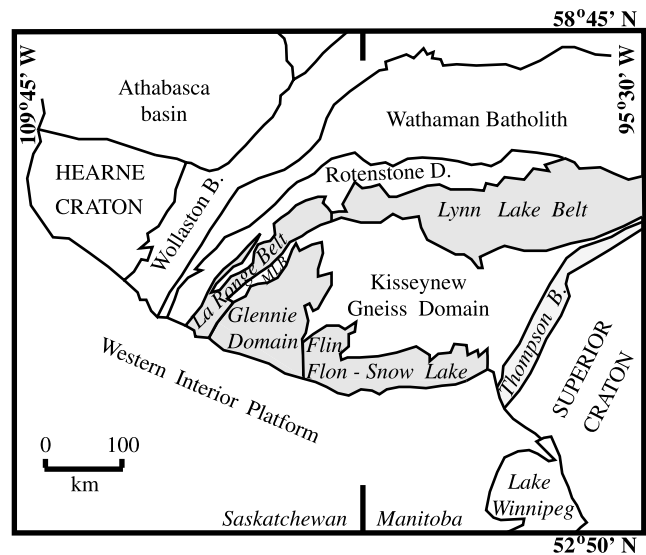


**Figure 1.** Map of the exposed Trans-Hudson Orogen and surrounding regions adapted from Lucas *et al.* [1996]. Geological domains are delineated. MLB indicates the metasedimentary McLean Belt. The main belts and domains which constitute the central Reindeer zone are shown.

hence different crustal structures. The northern volcanic belt consists of the Lynn Lake and La Ronge belts, two island arcs which were active near the Rae-Hearne craton. Following the geological and geochemical analysis of Maxeiner *et al.* [1999], we lump together the volcanic and plutonic rocks of the Glennie domain, the Flin Flon and Snow Lake Belts and their extensions beneath the Paleozoic sedimentary cover into a single southern volcanic belt. This belt was formed at large distance from the northern volcanic belt. The Flin Flon and Snow Lake Belts are made up of island arc and back arc volcanic and plutonic assemblages, as well as metamorphosed alluvial sediments. The Glennie Domain contains greenstone formations in a predominantly granitic terrain. A third unit, called the Central Gneiss domain, includes the metasedimentary rocks of the Kisseynew domain and the McLean belt. Finally, the fourth unit is the Thompson belt at the eastern edge of the THO, against the Superior province. This belt has no juvenile crust and is made of Paleoproterozoic continental rift margin rocks (Ospwagan group) and reworked Superior craton gneisses [Bleeker, 1990].

[7] Seismic refraction and reflection studies show that crustal thickness varies between <38 and >50 km in the THO [Nemeth *et al.*, 1996]. Such variations are associated with small Bouguer gravity anomalies, indicating that crustal structure and average density are laterally variable. Studies of the coherence between Bouguer gravity and topography suggest that the elastic lithospheric thickness varies between 40 and 80 km in the central part of the Canadian Shield but that it can exceed 120 km, in particular beneath parts of the THO [Wang and Mareschal, 1999].

## 3. New Heat Flow Determinations

### 3.1. Measurement Methods

[8] Heat flow and heat production data have been obtained at 17 new sites in the THO (Figure 2). The heat

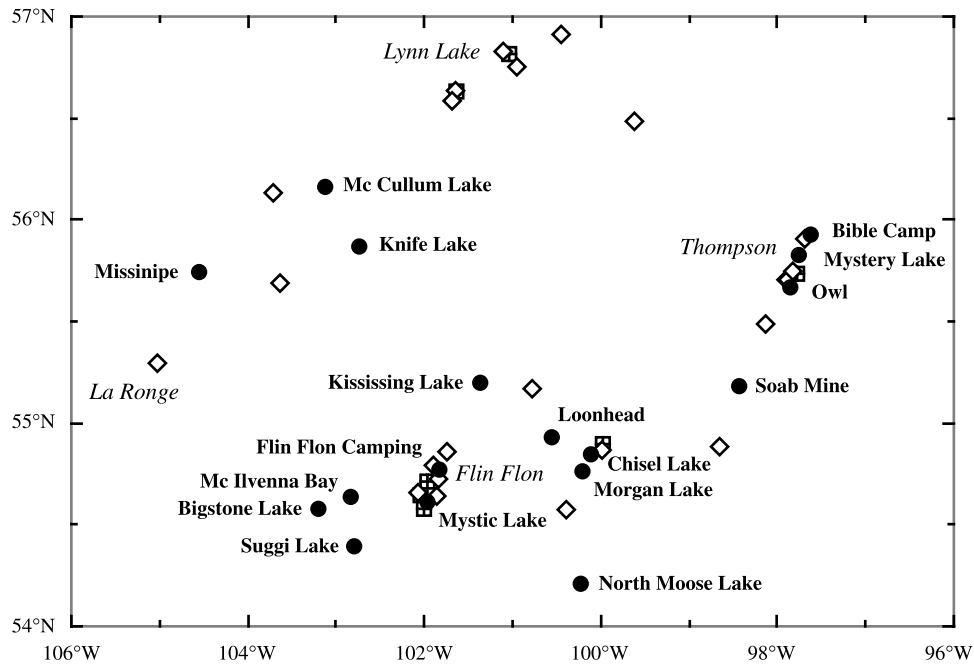


**Figure 2.** Geographical locations of heat flow sites in the Trans-Hudson Orogen. Circles correspond to the new sites of this paper. Previously published data are shown by diamonds [Mareschal *et al.*, 1999a, and references therein] and crossed squares [Drury, 1985, and references therein]. Major cities are shown in italics.

flow  $Q$  is determined from the measurements of the temperature gradient in boreholes and of the conductivity of rock samples:

$$Q = k \frac{\partial T}{\partial z}, \quad (1)$$

where  $k$  is the thermal conductivity,  $T$  is temperature, and  $z$  is depth. Measurement procedures were described by Mareschal *et al.* [1989] and Pinet *et al.* [1991]. Whenever possible, several boreholes separated by a few hundred meters are logged to obtain one heat flow determination. Temperature measurements are made at 10 m intervals in each borehole with a thermistor calibrated for a precision of 0.005 K. Stable temperature gradients were obtained over several hundreds of meters (Figures 3, 4, 5, 6, and 7). For each drill hole, core samples were collected and the thermal conductivity was measured by the divided bar method [Misener and Beck, 1960]. A single conductivity determination relies on five measurements on samples of thicknesses between 2 and 10 mm. This procedure allows the detection of sample-scale variations of mineralogy unrepresentative of the large-scale average rock composition.

[9] We have established the following criteria to rate the reliability of our heat flow measurements [Pinet *et al.*, 1991]. We divide the temperature profile for each borehole in subintervals within which the heat flow is calculated. The standard deviation is determined for all the heat flow values obtained. The sites rated A consist either of several boreholes deeper than 300 m giving consistent (within one standard deviation) heat flow values or a single borehole deeper than 700 m where the heat flow is stable over more than 300 m. Sites where the heat flow is less consistent

between boreholes or where the heat flow is obtained from a single borehole shallower than 600 m are rated B. Sites consisting of shallow (<300 m) boreholes or where differences between boreholes are larger than two standard deviations are rated C.

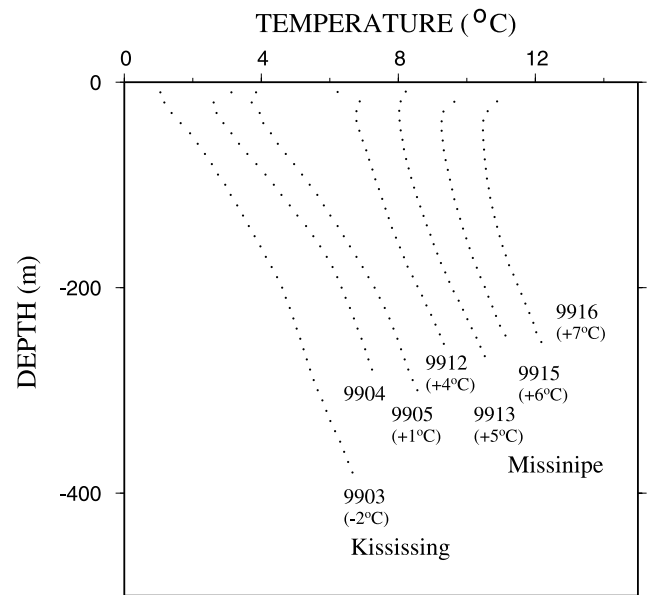


**Figure 3.** Temperature-depth profiles measured in the Kisseynew Domain and in the McLean Belt. The temperature profiles are shifted horizontally as indicated for clarity.

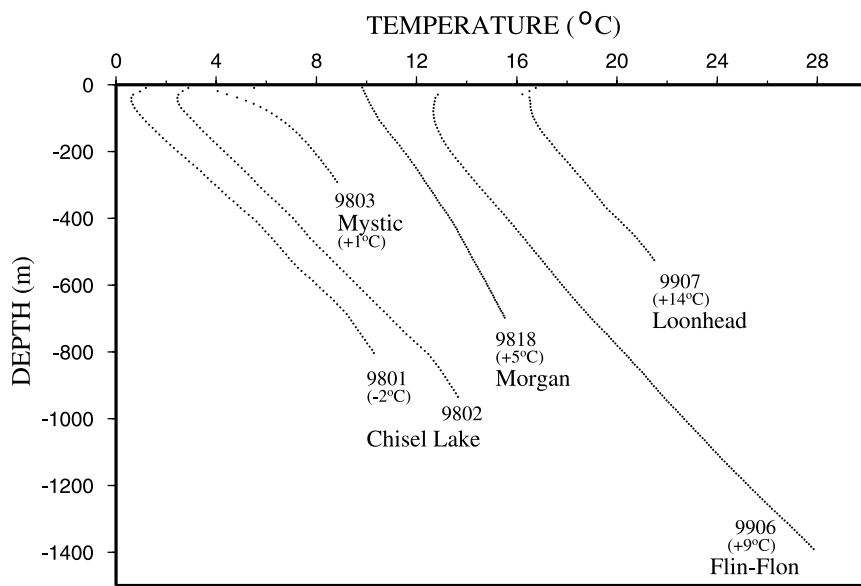


**Figure 4.** Temperature-depth profiles measured in the Flin Flon-Snow Lake Belt. The temperature profiles are shifted horizontally as indicated for clarity.

[10] A correction for the effect of Pleistocene glaciations was applied to the data based on the climatic model of *Jessop* [1971]. This was done for consistency with previously published values, although there is some debate on the importance of these corrections [*Sass et al.*, 1971; *Mareschal et al.*, 1999b]. In all sites the climatic correction is <10% of the measured value. In Appendix C, we discuss the climatic correction procedure for three sites close to large lakes (Mystic, Morgan, and Suggi), where horizontal variations of surface temperature perturb the temperature profile.

[11] Core samples from all the representative lithologies were collected for each borehole and their U, Th, and K concentrations were measured following the technique described by *Mareschal et al.* [1989]. Analytical errors on heat production measurements are typically <5% and are largest for low-radioactivity samples. For large-scale thermal models, the main source of uncertainty is the sampling. Comparison of mean heat production values from neighboring boreholes provides an estimate of this uncertainty. A summary of the new heat flow and heat production data is presented in Tables 1, 2, and 3. The geographical locations of

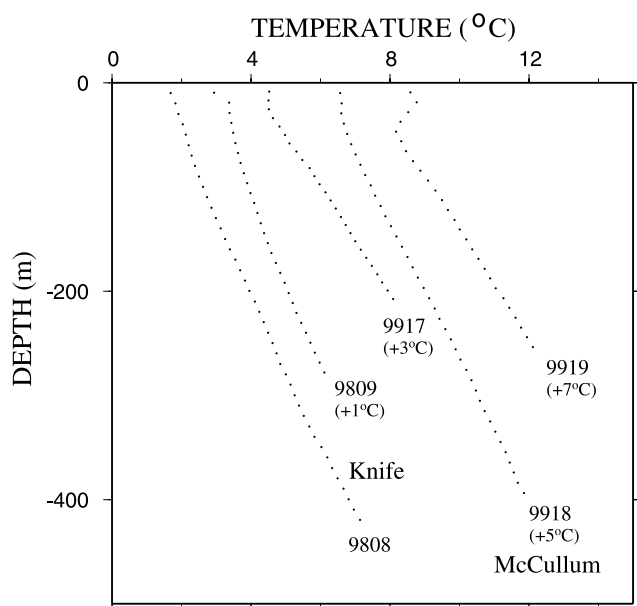


**Figure 5.** Temperature-depth profiles measured in the Glennie Domain. The temperature profiles are shifted horizontally as indicated for clarity.

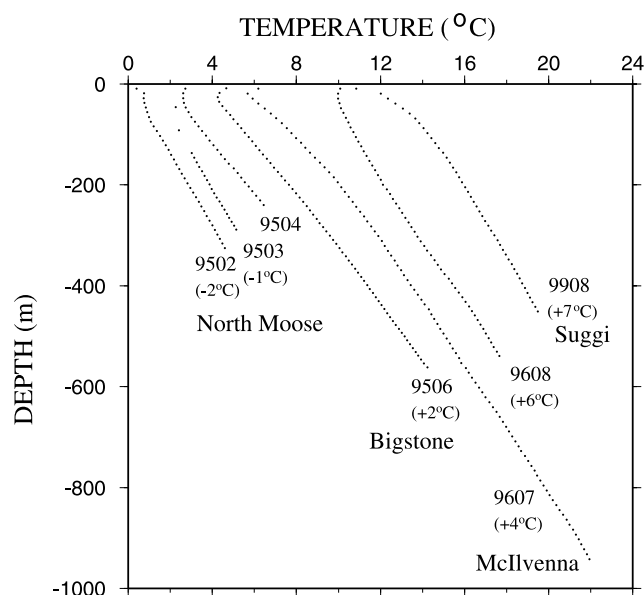


**Figure 6.** Temperature-depth profiles from the Paleozoic covered region. The temperature profiles are shifted horizontally as indicated for clarity.

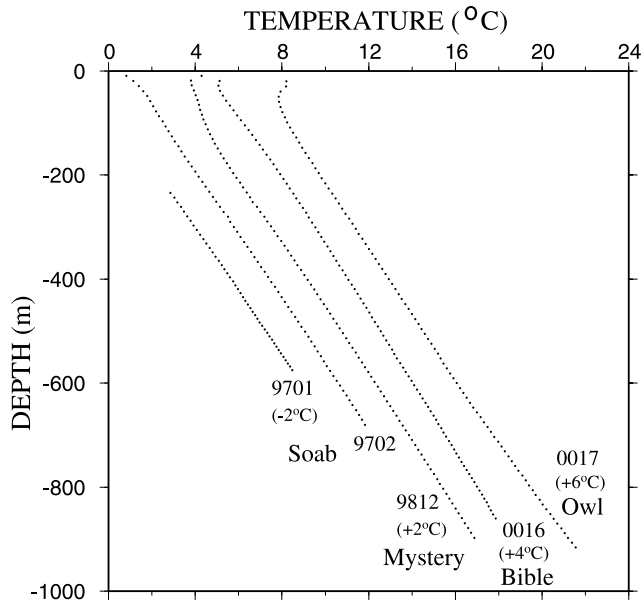


**Figure 7.** Temperature-depth profiles for the Thompson belt. For clarity, the profiles are shifted horizontally as indicated.

new heat flow sites and previously published data in the THO are shown in Figure 2. A description of each site follows.

### 3.2. Central Gneiss Domain

#### 3.2.1. Kississing Lake (Holes 9903, 9904, and 9905)

[12] This site is on the south flank of the metasedimentary gneisses of the Kisseynew, on a small island (1 km across)

on the wide Kississing lake. The perturbation caused by the lake is visible in the upper parts of the profiles (Figure 3). For this reason, we discarded the two shallowest boreholes (<300 m) and used only the lower part of the deepest borehole, where there is no effect of the lake. The value of  $34 \text{ mW m}^{-2}$  is close to the value of  $32 \text{ mW m}^{-2}$  obtained at Batty Lake, also in Kisseynew domain, some 80 km east of this site. The site is rated C.

#### 3.2.2. Missinipe (Holes 9912, 9913, 9915, and 9916)

[13] Four drill holes were logged through a sequence of interlayered arkose and arenite formations of the McLean belt. Marked perturbations due to the fairly steep topography affect the shallowest parts of the logs and disappear at depth. The boreholes can be grouped in two pairs located  $\sim 1$  km away from one another. Differences in gradient between these two groups (9912–9913 and 9915–9916) are almost offset by differences in thermal conductivity. The heat flow estimate of  $47 \text{ mW m}^{-2}$  is rated C.

### 3.3. Flin Flon-Snow Lake Belt

[14] We present values for five new sites in this well-sampled area (Figure 4). A sixth site, Leo Lake, is affected by heat refraction due to high thermal conductivity (Appendices A and B).

#### 3.3.1. Chisel Lake (Holes 9801 and 9802)

[15] Two deep boreholes through a sequence of metabasalts yield stable and consistent temperature gradients over 600 m. This site is rated A with a heat flow of  $39 \text{ mW m}^{-2}$ .

#### 3.3.2. Flin Flon Camping (Hole 9906)

[16] This very deep borehole (1400 m) is located east of the town of Flin Flon and penetrates metasedimentary and volcanic sequences. There is a small increase in temperature gradient with depth which is similar to that reported by *Sass*

**Table 1.** New Heat Flow Data<sup>a</sup>

Site Hole	Lat, North	Long West	Dip, deg	$\Delta h$ , m	$N_k$	$\langle k \rangle$ , $\text{W m}^{-1} \text{K}^{-1}$	$G$ , $\text{mK m}^{-1}$	$Q$ , $\text{mW m}^{-2}$	$\sigma_Q$ , $\text{mW m}^{-2}$	$\Delta Q$ , $\text{mW m}^{-2}$	$Q_c$ , $\text{mW m}^{-2}$
<i>Kisseynew Domain</i>											
Kississing Lake											
99-03	55 12 08	101 21 25	90	300–370	8	2.41	12.7	30.5	2.0	3.4	34 (C)
99-04	55 11 58	101 21 34	90	210–270	6	3.04	11.1				34.0
99-05	55 11 53	101 21 26	90	230–290	6	2.98	11.6				
<i>McLean Belt</i>											
Missinipe											
99-12	55 44 50	104 33 09	72	199–245	6	3.04	13.9	42.2	1.8	2.6	47 (C)
99-13	55 44 55	104 33 21	70	222–258	9	3.32	14.3	47.5	0.8	2.7	44.8
99-15	55 44 52	104 33 29	72	199–228	7	3.54	12.1	42.7	0.3	3.3	50.2
99-16	55 44 48	104 33 25	71	197–244	7	3.50	12.1	42.5	2.7	3.3	46.1
<i>Flin Flon-Snow Lake Belt</i>											
Chisel Lake											
98-01	54 50 44	100 06 35	84	200–794	15	2.90	13.0	37.7	2.9	2.6	39 (A)
98-02	54 50 48	100 06 24	84	200–924	18	2.84	12.7	36.2	3.0	2.2	40.3
Flin Flon Camping											
99-06	54 46 23	101 50 15	85	966–1391	23	3.57	13.2	40.0	2.1	0.9	38.4
Loonhead											
99-07	54 55 54	100 33 48	76	214–336	11	3.70	11.5	42.6	2.2	2.6	41 (A)
				461–517	11	4.05	10.8	43.6	1.6	3.2	40.9
Morgan Lake											
98-18	54 45 34	100 12 23	63	433–691	13	3.15	7.2	22.8	1.0	5.5	46 (B)
Mystic Lake											
98-03	54 36 57	101 58 09	73	133–282	5	3.00	11.3	33.9	2.1	5.2	45.8

<sup>a</sup>For each borehole we give the latitude, longitude, dip at the collar of the drill hole, vertical depth interval used for heat flow determination, number of conductivity samples measured, average thermal conductivity, average temperature gradient over the depth interval, mean heat flow, standard deviation, correction for postglacial warming, and adjusted heat flow. The quality of the heat flow value for each site is rated A, B, or C, as discussed in text.

**Table 2.** New Heat Flow Data Continued

Site Hole	Lat north	Long west	Dip, deg	$\Delta h$ , m	$N_k$	$\langle k \rangle$ , $\text{W m}^{-1} \text{K}^{-1}$	$G$ , $\text{mK m}^{-1}$	$Q$ , $\text{mW m}^{-2}$	$\sigma_Q$ , $\text{mW m}^{-2}$	$\Delta Q$ , $\text{mW m}^{-2}$	$Q_c$ , $\text{mW m}^{-2}$
<i>Glennie Domain</i>											
Knife Lake											30 (C)
98-08	55 52 08	102 44 25	90	200–320	10	2.02	13.2	26.6	2.0	1.4	28.0
				360–410	10	1.93	15.6	30.2	1.0	0.9	31.1
98-09	55 52 17	102 44 13	75	230–269	7	2.04	13.9	28.4	0.6	1.4	29.8
McCullum Lake											39 (B)
99-18	56 09 34	103 06 57	80	118–384	6	2.50	14.9	37.3	1.3	1.5	38.8
99-17	56 08 48	103 08 28	51	113–192	5	2.69	19.0				
99-19	56 08 55	103 08 35	70	113–244	5	2.66	18.6				
<i>Southern Margin (Beneath Paleozoic Cover)</i>											
Bigstone Lake											63 (B)
95-06	54 34 31	103 11 59	62	391–546	8	3.45	17.4	60.0	1.7	3.3	63.3
95-04	54 34 31	103 11 59	70	84–231	8	3.58	19.9				
McIlvenna Bay											41 (A)
96-07	54 38 16	102 49 42	77	302–932	10	2.49	15.7	39.2	3.1	2.7	41.9
96-08	54 38 09	102 49 43	77	450–531	7	2.49	14.6	36.5	1.3	3.3	39.8
Suggi Lake											54 (B)
99-08	54 23 36	102 48 02	77	175–442	9	3.31	14.1	46.7	2.1	7.0	53.7
North Moose Lake											60 (B)
95-02	54 12 49	100 13 47	70	112–351	6	3.97	13.7	54.6	2.6	3.8	58.3
95-03	54 12 49	100 13 47	66	216–281	6	3.95	14.6	57.5	1.7	3.5	61.0
<i>Thompson Belt</i>											
Mystery Lake											52 (A)
98-12	55 49 40	97 45 40	70	448–888	15	3.23	15.5	49.9	1.1	1.7	51.6
Soab Mine											50 (A)
97-01	55 11 30	98 24 40	70	349–568	7	3.05	16.2	49.5	1.8	1.8	51.3
97-02	55 10 14	98 27 28	75	300–670	9	3.00	15.9	47.7	2.0	1.7	49.5
Bible Camp											54 (B)
00-16	55 55 32	97 37 09	72	578–813	13	3.46	14.9	51.7	2.2	1.8	53.5
Owl											52 (A)
00-17	55 40 17	97 51 35	82	226–907	13	3.10	16.5	51.1	2.1	1.1	52.2

*et al.* [1971] for a site 15 km to the south. The heat flow value of  $41 \text{ mW m}^{-2}$  is rated A.

### 3.3.3. Loonhead Lake (Hole 9907)

[17] This borehole is drilled in felsic volcanic sequences and intersects a thin sloping low conductivity volcanic layer. This generates heat refraction effects which are perfectly reproduced by calculation (Appendix B). The model indicates which depth intervals may be used for heat flow determination (Table 1). The resulting heat flow value is rated B.

### 3.3.4. Morgan Lake (Hole 9918)

[18] This deep borehole intersects sequences of dacitic and intermediate felsic tuffs. It lies at the edge of a large lake and requires a special procedure for climatic correction (Appendix C). The shallow part of the temperature log is affected by the lake. In the deeper part, the gradient is stable and small ( $7.2 \text{ mK m}^{-1}$ ). The resulting heat flow value,  $28 \text{ mW m}^{-2}$  is the lowest one in the Flin Flon-Snow Lake Belt and is rated B.

### 3.3.5. Mystic Lake (Hole 9803)

[19] This shallow borehole is situated near the shore of a lake and intersects mafic volcanic rocks. The heat flow value of  $39 \text{ mW m}^{-2}$  based on a single borehole <300 m is rated C.

## 3.4. Glennie Domain

### 3.4.1. Knife Lake (Holes 9808 and 9809)

[20] These two boreholes are drilled in sequences of felsic, mafic, and intermediate volcanics. Differences in gradient between the identical upper sections of the two

boreholes and the deepest section of hole 9808 are partly offset by differences in thermal conductivity. The resulting value of  $30 \text{ mW m}^{-2}$  is rated C (Figure 5 and Table 2).

### 3.4.2. McCullum Lake (Holes 9917, 9918, and 9919)

[21] These boreholes intersect typical greenstone volcanics and pelitic metasediments enriched in radioactive elements (Table 3). Two shallow boreholes (9917 and 9919) are located very close to the lake and their temperatures are obviously perturbed. The third, and deepest, borehole, located  $\sim 3 \text{ km}$  away from lake shores, yields a stable temperature gradient over 250 m. The heat flow value of  $39 \text{ mW m}^{-2}$  is rated B.

## 3.5. Southern Margin at the Edge of the Paleozoic Cover

[22] The southern part of the THO has been covered by Phanerozoic rocks of the Western Canada Sedimentary Basin. We have carried out measurements in four sites located very close to the Precambrian-Phanerozoic contact, where the main lithological units of the THO have been extended southward [Leclair *et al.*, 1997]. All the drill holes (Figure 6) penetrate through basement and heat production was calculated for basement rock samples only.

### 3.5.1. Bigstone Lake (Holes 9504 and 9506)

[23] This site is located in the Glennie domain. The drill holes penetrate metamorphic rocks derived from rhyolitic volcanics. Temperature gradients in the two holes are identical in the upper 250 m and are perturbed by the neighboring lake. The equilibrium heat flow was determined from the deep part of borehole 9506 where heat

**Table 3.** Heat Production Measurements for 20 New Sites in the THO<sup>a</sup>

Site (Hole)	Main Lithology	Number of Samples	U, ppm	Th, ppm	K, %	Heat Production, $\mu\text{W m}^{-3}$
Kississing Lake (9903, 9904, 9905)	gneiss	<i>Kisseynew</i> 17	2.22	3.53	1.28	0.93 (0.08)
Missinipe (9912, 9913, 9915, 9916)	arkose/arenite	<i>McLean Belt</i> 19	3.97	11.15	2.90	2.06 (0.18)
Knife Lake (9808, 9809)	mixed volcanics	<i>Glennie Domain</i> 11	0.93	2.12	0.88	0.47 (0.10)
McCullum Lake (9917, 9918, 9919)	mafic volcanics	6	1.47	3.66	1.49	0.77 (0.19)
	pelitic sediments	5	2.11	5.19	1.70	1.06 (0.24)
Bigstone Lake (9506)	felsic metavolcanics	<i>Southern Margin</i> 15	1.45	1.63	1.49	0.62 (0.03)
McIlvenna Bay (9607, 9608)	schists	6	3.28	6.13	2.42	1.49 (0.21)
Suggi Lake (9908)	felsic gneiss	5	1.07	1.57	1.49	0.52 (0.03)
North Moose Lake (9502, 9503)	schists/gneiss	9	1.34	1.78	1.93	0.64 (0.09)
Chisel Lake (9801, 9802)	metabasalt	<i>Flin Flon-Snow Lake Belt</i> 20	0.64	1.65	0.77	0.35 (0.06)
Flin Flon Camping (9906)	basalt	9	0.45	0.54	0.45	0.19 (0.03)
Leo Lake (9806, 9807, 9909)	felsic volcanics	24	1.01	3.23	1.23	0.60 (0.03)
Loonhead (9907)	felsic volcanics	9	1.16	3.03	1.05	0.60 (0.13)
Morgan Lake (9818)	felsic volcanics	15	0.64	1.18	0.94	0.33 (0.03)
Mystic Lake (9803)	mafic volcanics	3	0.56	1.20	1.00	0.32 (0.00)
Mystery Lake (9812)	granodiorite	<i>Thompson Belt</i> 15	2.39	3.62	2.04	1.05 (0.11)
Soab Mine (9701, 9702)	metasediments	6	0.81	9.05	2.34	1.05 (0.21)
Bible Camp (0016)	metasediments	9	0.73	9.23	2.32	1.04 (0.18)
Owl (0017)	metasediments	16	1.17	11.41	2.14	1.29 (0.17)
Cluff Lake (9920)	altered gneiss	<i>Athabasca Basin</i> 6	2.45	10.62	2.88	1.63 (0.26)
Shea Creek (9922, 9923)	stones	11	1.21	3.31	0.38	0.58 (0.08)

<sup>a</sup>At each site the dominant lithology, the number of samples used, the averaged heat production, and the standard error are given.

flow does not vary with depth. The heat flow value of 63  $\text{mW m}^{-2}$  is rated B.

### 3.5.2. McIlvenna Bay (Holes 9607 and 9608)

[24] These two deep boreholes are located in the southern extent of the Hanson Lake block in the Flin Flon belt [Leclair *et al.*, 1997; Maxeiner *et al.*, 1999] where Archean basement windows are identified [Ashton *et al.*, 1999]. They penetrate sequences of schists interlayered with gabbros and basalts. They yield stable and consistent temperature gradients. The site is rated A, with a resulting heat flow value of 41  $\text{mW m}^{-2}$ .

### 3.5.3. Suggi Lake (Hole 9908)

[25] This 450 m deep drill hole is also located in the Hanson Lake block, south of the McIlvenna Bay site. The temperature log exhibits perturbations due to the neighboring lake in its upper part (<200 m) and has a stable gradient below. The climatic correction procedure for this site is detailed in Appendix B. The high heat flow value of 54  $\text{mW m}^{-2}$  is rated B.

### 3.5.4. North Moose Lake (Holes 9502 and 9503)

[26] The boreholes penetrate the southern extent of the Snow Lake volcanic assemblage [Leclair *et al.*, 1997]. From the two temperature logs, we obtain a high heat flow value of 60  $\text{mW m}^{-2}$ , which is rated B.

## 3.6. Thompson Belt

### 3.6.1. Soab Mine (Holes 9701 and 9702)

[27] Two deep boreholes in metasedimentary sequences are located ~4 km apart near the now abandoned Soab

Mine, ~75 km south of the city of Thompson. They yield stable and identical temperature gradients (Figure 7). The heat flow value of 50  $\text{mW m}^{-2}$  is very reliable and rated A.

### 3.6.2. Mystery Lake (Hole 9812)

[28] This deep borehole in granodioritic rocks yields a stable temperature gradient and the reliable heat flow determination is rated A. The heat flow value of 52  $\text{mW m}^{-2}$  is almost identical to that obtained 10 km to the north at Moak Lake (53  $\text{mW m}^{-2}$ ) [Guillou-Frottier *et al.*, 1996].

### 3.6.3. Bible Camp (Hole 0016)

[29] This deep borehole is the northernmost site of the Thompson belt, 4 km north of Moak Lake, and is drilled in metasedimentary sequences. The heat flow value of 54  $\text{mW m}^{-2}$ , rated B, is very similar to those of Mystery Lake and Moak Lake.

### 3.6.4. Owl (Hole 0017)

[30] This deep borehole is located 3 km away from the Birchtree Mine site [Guillou-Frottier *et al.*, 1996]. It penetrates metasedimentary rocks and yields stable temperature gradient over 700 m. The heat flow value of 52  $\text{mW m}^{-2}$  is rated A.

## 4. Distribution of Heat Flow in the THO

[31] The new heat flow map for the Trans-Hudson Orogen (Figure 8), which now includes a total of 45 determinations confirms the main heat flow trends described by Mareschal *et al.* [1999a]. Heat flow statistics for the four THO domains differ significantly (Table 4).

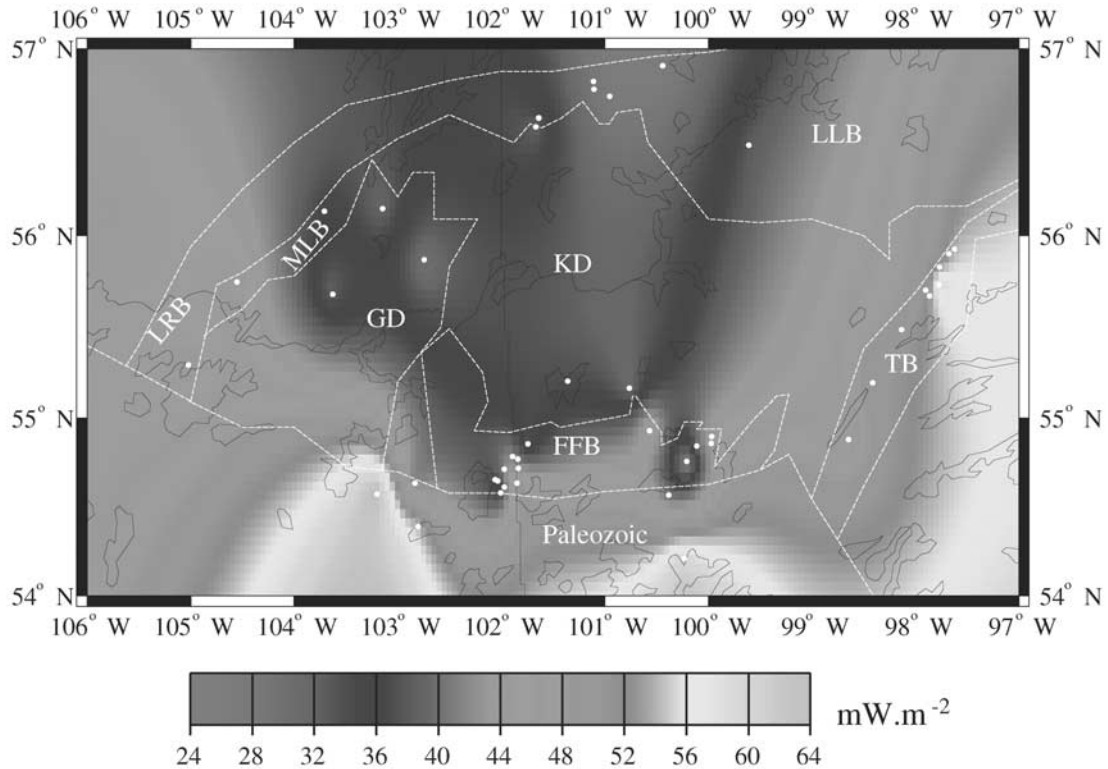


**Figure 8.** Heat flow map of the Trans-Hudson Orogen. White dots are the heat flow sites. The main belts of the Reindeer tectonic zone are outlined: Glennie Domain (GD), Flin Flon-Snow Lake Belt (FFB), Kisseynew Domain (KD), Lynn Lake Belt (LLB), La Ronge Belt (LRB), McLean Belt (MLB). The Thompson belt (TB) and the Paleozoic Cover are also indicated. See color version of this figure at back of this issue.

[32] Superimposing the geological and heat flow maps (Figures 1 and 8) suggests a strong correlation between the heat flow field and the surface geology, which is supported by heat flow statistics (Table 4). The heat flow pattern is essentially that of a low heat flow area, including the Lynn Lake Belt and the Kisseynew Domain, an ancient marginal basin, grading into higher heat flow belts involving older Archean crust, the largely hidden Sask craton beneath the southern volcanic belt, the Rae-Hearne craton west of the northern volcanic belt and the Superior craton beneath the Thompson belt. As discussed below, there is a negative correlation between heat flow and the proportion of juvenile material in the crustal column. Juvenile Proterozoic crust is exposed in the southern and northern volcanic belts and in the central gneiss domain, and is associated with lower heat flow values than those in the Thompson belt, which is made up entirely of reworked Archean rocks.

**4.1. Short-Wavelength Variations in the Flin Flon-Snow Lake Belt**

[33] This belt is a mosaic of distinct assemblages brought together at a relatively early stage in the tectonic evolution of the THO [Lucas *et al.*, 1996]. Four main assemblages are recognized: ocean floor, oceanic plateau/ocean island, juvenile oceanic arc and evolved arc. 15 heat flow values are now available for this belt, within a range of 28 to 51 mW m<sup>-2</sup> (Figure 9). The highest value (51 mW m<sup>-2</sup> at the Schist Lake site) occurs within less than 15 km of two sites

with lower heat flow (37, 39 mW m<sup>-2</sup>). Similarly, the lowest value (28 mW m<sup>-2</sup>, at the Morgan Lake site), is found <20 km away than sites with higher heat flow values (39, 41 mW m<sup>-2</sup>). Such small-scale heat flow variations can only be due to changes of heat production in the upper crust. Surface rocks are mostly juvenile mafic volcanics with small U and Th concentrations and a mean heat production of 0.3 ± 0.2(SD) μW m<sup>-3</sup>. Over a total crustal thickness of 38–40 km [Pandit *et al.*, 1998; Zelt and Ellis, 1999], such rocks can account neither for the mean heat flow value of 41 mW m<sup>-2</sup> nor for the magnitude of heat flow variations. This implies that the surficial volcanics rest on more radiogenic heterogeneous basement.

[34] Independent geophysical surveys in the Flin Flon-Snow Lake Belt indicate the presence of numerous small-scale structures distributed throughout the upper crust over a

**Table 4.** Mean Heat Flow and Heat Production in Four Different Belts of the Trans-Hudson Orogen

	$\langle Q \rangle$ , mW m <sup>-2</sup>	$\sigma_Q$	$N_Q$	$\langle A \rangle$ , μW m <sup>-3</sup>	$\sigma_A$	$N_A$
Northern volcanic belt	34 ± 2.3	7	9	0.81 ± 0.15	0.45	9
Southern volcanic belt	42 ± 1.8	8	23	0.45 ± 0.07	0.32	22
Central gneiss domain	37 ± 3.0	6	4	1.02 ± 0.31	0.63	4
Thompson belt	52 ± 1.2	4	9	0.98 ± 0.07	0.19	8
Trans-Hudson (whole data set)	42 ± 1.4	9	45			

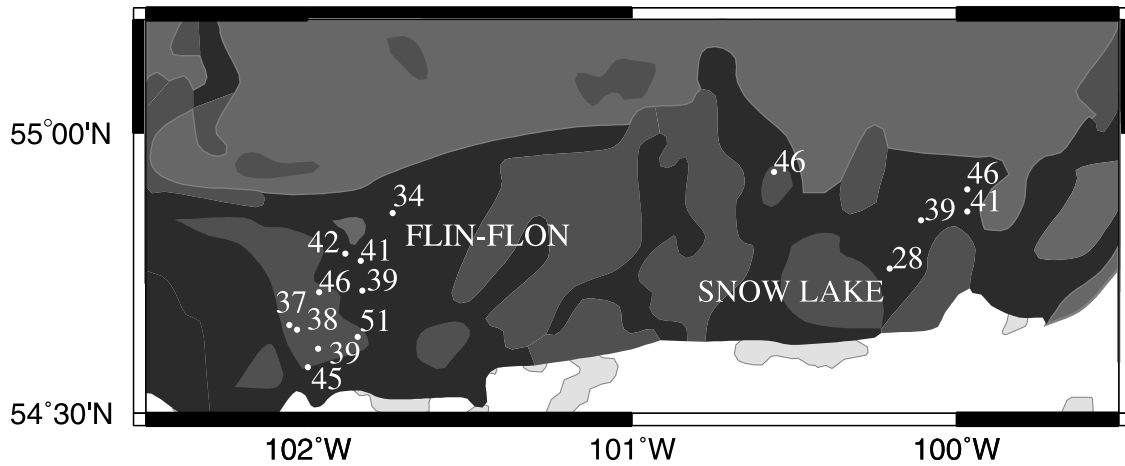


**Figure 9.** Heat flow values displayed on a simplified geological map of the Flin Flon-Snow Lake Belt. Dark gray, volcanic rocks; intermediate grey, granitoid rocks; light gray, metasedimentary rocks. Modified from *Wheeler et al.* [1997].

thickness of  $\sim 20$  km [Ferguson *et al.*, 1999]. We have measured the radiogenic heat production of rocks other than primitive lavas. Missi Group continental sediments (1.85 Ga), which occur as folded lenses at various locations, have a heat production of  $1.1 \mu\text{W m}^{-3}$ . Similarly, schists of unknown age from the deepest parts of the Chisel Lake boreholes, below the surficial basaltic rocks, have a heat production of  $1.0 \mu\text{W m}^{-3}$  (Table 5). Variable amounts of such rocks in the upper 20 km of the crust can account for both the magnitude and small-wavelength of heat flow variations in the Flin Flon-Snow Lake Belt.

#### 4.2. High Heat Flow at the Margin of the Paleozoic Cover

[35] Five heat flow values are now available through crystalline basement beneath the sedimentary cover a few kilometers south of the southern belt margin: four new values reported here (Table 2) and one older measurement at the Reed Lake site [Guillou-Frottier *et al.*, 1996]. The mean value for these five sites is  $52 \text{ mW m}^{-2}$ , which is significantly larger than the average values for the southern belt as well as for the whole THO ( $42 \pm 1.8 \text{ mW m}^{-2}$  and  $42 \pm 1.4 \text{ mW m}^{-2}$ , respectively, Table 4). The drill holes at these sites go through gneiss and metavolcanic rocks of evolved felsic compositions with higher radioelement concentrations than elsewhere in the southern belt (Table 3). The average heat production of surface rocks  $0.7 \pm 0.2 \mu\text{W m}^{-3}$ , compared to a mean value of  $0.4 \pm 0.1 \mu\text{W m}^{-3}$  for the other sites in the southern belt. However, this difference alone would require a thickness larger than 20 km to account for the difference in heat flow. Because this depth is not consistent with seismological estimates [Zelt and Ellis, 1999], crust must be more radioactive below the surficial layer.

[36] The southern volcanic belt is characterized by higher heat flow values than the other juvenile belts of Proterozoic age in the THO. In a previous paper [Mareschal *et al.*, 1999a], we have emphasized that juvenile THO crustal material is not radiogenic, probably because magmatic differentiation processes did not proceed for sufficiently long. Therefore the radiogenic crustal material at depth in

the southern belt must be older than Proterozoic. This is consistent with the presence of the Archean Sask craton in the southern part of the THO [Lucas *et al.*, 1993; Lewry *et al.*, 1994; Hajnal *et al.*, 1995]. The heat flow data suggest that the thickness of Sask crust increases toward the south. Crystalline basement rocks beneath the sedimentary cover have been extensively sampled further south in the western platform of Saskatchewan [Burwash and Cumming, 1976]. These rocks have average *U* and *Th* concentrations of 4.1 and 21.1 ppm, respectively [Burwash and Cumming, 1976]. Using a standard ratio *K/U* equal to  $10^4$ , the average heat production is  $2.9 \mu\text{W m}^{-3}$ , which is one order higher than the average heat production of juvenile rocks in the THO. Such rocks could account for the larger heat flow values of the southern volcanic belt.

#### 4.3. Northern Part of the Thompson Belt

[37] The Thompson belt is characterized by high heat flow and heat production values (Table 4). A heat flow profile along the strike of the belt (Figure 10) has two significant features: a long-wavelength south-north increase from  $45 \text{ mW m}^{-2}$  to  $54 \text{ mW m}^{-2}$  and two anomalously high heat flow values near the town of Thompson. These are due to local heat refraction effects by high-conductivity lenses [Guillou-Frottier *et al.*, 1996], as explained in Appendix B and hence have no bearing on the large-scale thermal structure of the Thompson belt.

[38] The long-wavelength heat flow variation along the Thompson belt can only be attributed to changes of crustal structure. Such changes have also been established by seismic and magnetotelluric studies [White *et al.*, 1999]. Together with geological constraints, these studies have led to the following crustal models. Proterozoic rocks of the

**Table 5.** Other Heat Production Data

Lithology	Number of Samples	U, ppm	Th, ppm	K, %	A $\mu\text{W m}^{-3}$
Missi sediments	13	2.13	5.37	1.83	1.09
Schists	4	1.99	6.13	1.06	1.04

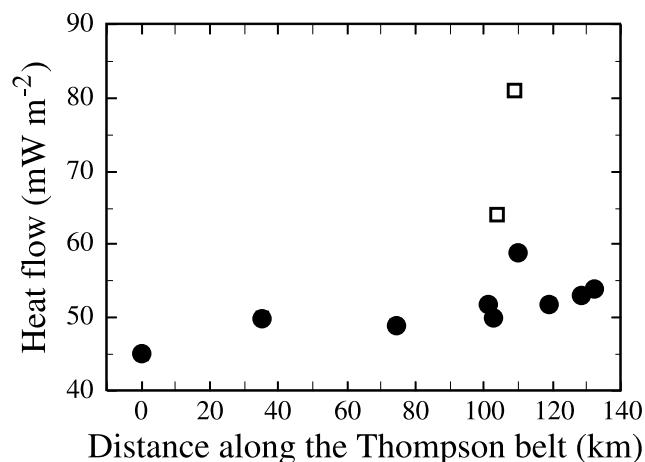


**Figure 10.** Heat flow variations along the Thompson belt. Individual heat flow values are projected onto a line connecting the southernmost site at 54°52'N, 98°38'W to the northernmost site at 55°55'N, 97°37'W (see Figure 8). White squares refer to sites in high-conductivity bodies affected by local heat refraction (see text).

Kisseynew dip beneath the surficial metasediments in the southern part of the profile and are absent from the northern part which is made exclusively of Archean protoliths. The heat flow data support this interpretation because Proterozoic rocks of the THO are poor in radioelements, as discussed above.

## 5. Large-Scale Implications

### 5.1. Heat Flow as a Function of Age

[39] A cursory analysis shows that the THO heat flow field cannot be distinguished from those of the Archean Superior Province and of the younger Proterozoic Grenville Province. These three provinces are now well sampled and their bulk heat flow statistics are almost identical, with mean values and standard deviations of 41–42 and 9–11 mW m<sup>-2</sup> (Table 4) [Mareschal *et al.*, 1999a]. However, the THO lumps together very different types of crust and does not compare with these other provinces from a petrological perspective. In the THO, only two belts, the northern volcanic belt and the Central Gneiss Domain, can be described as truly Proterozoic in age, made of crustal material derived from the mantle by partial melting at that time. In contrast, the southern volcanic and Thompson belts consist mostly of Archean rocks which have been either underthrust beneath younger volcanics or recycled through sedimentation and metamorphism at the Superior craton margin. Heat flow in the juvenile Proterozoic belts is lower than in the others. Implications for the mechanisms of crustal growth and differentiation have been discussed by Mareschal *et al.* [1999a].

### 5.2. Large-Scale Heat Flow Variations in North America

[40] On a west-to-east traverse starting near the center of the Canadian Shield and ending at the coastline, there is no systematic heat flow trend. This is clear from the bulk statistics of the Superior, THO and Grenville provinces.

Furthermore, areas with small heat flow values of 25–28 mW m<sup>-2</sup> are found across the Shield, in the THO near Lynn Lake in the northern volcanic domain, near the Grenville front [Mareschal *et al.*, 2000a] and at Voisey Bay, Labrador [Mareschal *et al.*, 2000b]. Thus the surface heat flow field does not define any systematic spatial pattern on the scale of the whole continent. Heat flow values are larger in younger provinces to the west or to the south, but these are accounted for by more radiogenic crust in the Appalachians [Jaupart and Mareschal, 1999] and recent thermal events in the Cascades [Blackwell *et al.*, 1990] and Colorado [Decker *et al.*, 1980].

[41] Using a worldwide data set, Nyblade and Pollack [1993] have proposed that Archean and Proterozoic provinces are characterized by different average heat flow values and have attributed this difference to variations of lithosphere composition and thickness. They distinguished between the stabilization of a lithospheric block and subsequent thermal or tectonic events which are recorded in surface rocks but which might not have affected the deeper part of the lithosphere. They also suggested that when allochthonous terrains are present, Proterozoic mantle lithosphere can only be found at some distance (~400 km) from the surface contact. In Canada, no Proterozoic province could be used to test this hypothesis because their half width is always less than 300 km. The Grenville province, for example, contains allochthonous terranes thrust over Archean basement near its contact with the Archean Superior Province. This is indeed reflected in the surface heat flow field which shows no significant change across this contact [Mareschal *et al.*, 2000a]. Furthermore, the Grenville province is <500 km wide. In the THO, the southern volcanic belt is in part thrust over Archean basement [Lucas *et al.*, 1996]. The THO is surrounded by Archean cratons and is nowhere wider than about 600 km. Thus it is not surprising that, in the Canadian Shield, heat flow data show no differences between Proterozoic and Archean provinces. Because of the architecture of the Precambrian in North America, it may well prove impossible to find a Proterozoic lithospheric block of sufficient size to test the model by Nyblade and Pollack [1993].

[42] In order to use heat flow data for studies of deep lithospheric structure, one must account for crustal heat production which is a large component of the measurements. This key step is made difficult by the very heterogeneous nature of continental crust and by the scarcity of lower crustal samples, as discussed at length by Rudnick and Fountain [1995] and by Jaupart *et al.* [1998]. An additional difficulty is that the mantle heat flow estimate is small and hence is affected by large residual errors. For example, Guillou *et al.* [1994] and Jaupart *et al.* [1998] have used several constraints on crustal structure and composition to bracket the mantle heat flow beneath the Canadian Shield between 7 and 15 mW m<sup>-2</sup>. The relative uncertainty is therefore very large. Furthermore, the uncertainty of individual heat flow measurements is seldom less than ~2 mW m<sup>-2</sup>. Thus “geological” as well as instrumental noise hampers our ability to detect variations of deep lithospheric structure. Nevertheless, heat flow data do provide powerful constraints when combined with dynamical arguments and considerations of heat transport mechanisms [Jaupart *et al.*, 1998; Jaupart and Mareschal, 1999].

As shown by these studies, the mantle heat flow value is most useful and we now focus on tightening its range.

### 5.3. Mantle Heat Flow

[43] Removing the variable contribution of crustal heat generation from heat flow measurements is impossible without knowledge of the lower crustal composition. To alleviate this difficulty, many authors have relied on an empirical linear relationship between heat flow and heat production [Birch *et al.*, 1968], even though the extrapolation procedure over the whole crust is highly questionable [England *et al.*, 1980; Jaupart, 1983]. In the THO, it is useless to discuss this problem further because there is no such relationship [Mareschal *et al.*, 1999a]. For example, values of heat flow and heat production in the northern and southern volcanic belts are anticorrelated (Table 4).

[44] Conditions in the convecting mantle below continents remain largely unknown, however variations of heat supply at the base of the lithosphere over length scales of a few hundred kilometers would not be detectable at the surface because of lateral diffusion. Thus the heat flow at the Moho, called mantle heat flow for simplicity, can be taken as constant over the whole THO province. Heat flow variations can only be due to the presence of different types of crust, and we focus on areas with low heat flow values, where the total crustal heat production is small.

[45] In the THO, the heat flow is lowest near the town of Lynn Lake in the northern volcanic belt. There, the local average value for a region  $\sim 50$  km wide, is  $28 \text{ mW m}^{-2}$ . According to current interpretations, the northern volcanics formed when the Kiseynew back arc basin was thrust beneath an island arc at the edge of the Rae-Hearne craton. Oceanic crust has been identified at the suture [Zwanzig *et al.*, 1999]. Crustal thickness exceeds 50 km at the southern margin of the belt [Nemeth *et al.*, 1996; Nemeth and Hajnal, 1997] and decreases abruptly southeast of the Lynn Lake area, which may mark the edge of the subducted Kiseynew oceanic slab [White *et al.*, 2000]. Assuming that the main crustal structures are parallel to the strike of the belt, the Lynn Lake area has thinner crust ( $\sim 40$  km) than the suture and the Kiseynew domain. Surface outcrops throughout the northern volcanic belt allow sampling at different structural levels and metamorphic grades in the crustal sequence [Baldwin *et al.*, 1987]. Thus the average heat production of surface rocks ( $0.8 \mu\text{W m}^{-3}$ , Table 4) provides an estimate of the depth average of heat production of the volcanic sequence as well. This sequence is  $\sim 12$  km thick [White *et al.*, 2000] and hence contributes  $\sim 10 \text{ mW m}^{-2}$ . We have no information on the composition of the lower crustal sequence which is at least 28 km thick, and hence cannot estimate its radiogenic heat production. However, no crustal assemblage has heat production lower than  $0.05 \mu\text{W m}^{-3}$ , including oceanic crust. Taking this value as a lower bound, we obtain an upper bound of  $16 \text{ mW m}^{-2}$  for the mantle heat flow beneath the Lynn Lake area.

[46] The other low heat flow area in the THO is the central Gneiss domain (Table 4), where four heat flow determinations are available. The thickness of metasediments in the Kiseynew is about 20 km [White *et al.*, 2000]. For a mean heat production of  $1.0 \mu\text{W m}^{-3}$  (Table 4), they may contribute as much as  $20 \text{ mW m}^{-2}$ . Thus the heat flow at the base of the metasedimentary layer may be as low as

$17 \text{ mW m}^{-2}$ . The crustal thickness is  $\sim 50$  km [White *et al.*, 2000], and the same argument as above leads to an upper bound of  $15 \text{ mW m}^{-2}$  for the mantle heat flow.

[47] Errors on these estimates are difficult to assess. The Kiseynew Domain was a small oceanic basin (possibly back arc), implying that the lower crust is made up of oceanic basement depleted in radioelements. The Lynn Lake area is probably underlain by the same basement. Thus, in both cases, the lower crust contributes a very small fraction of the surface heat flow. Errors can only come from an incorrect estimates of thickness and average heat production in the upper crustal layer. We note that two independent calculations involve different values of surface heat flow, upper layer thickness and heat production, and yet lead to almost the same result for the mantle heat flow. Known differences of heat production and thickness of the upper crust account for most of the observed heat flow difference.

## 6. Mantle Heat Flow and Crustal Temperatures in the Thompson Area

### 6.1. Melting Conditions in the Continental Crust

[48] When the THO finally stabilized, about 1.8 Ga, radiogenic isotope concentrations and heat production, and hence crustal temperatures, were larger than today. High heat flow values imply high crustal heat production and one useful constraint is that melting conditions were not reached in the crust. In common crustal rock types, the amount of melt formed in fluid-absent conditions becomes significant at temperatures above  $800^\circ\text{C}$  [Clemens and Vielzeuf, 1987]. In many natural metamorphic crustal rocks, dehydration melting begins at temperatures ranging from  $850^\circ\text{C}$  at 300 MPa to  $930^\circ\text{C}$  at 1.5 GPa [Patino Douce and Beard, 1995]. In biotite, plagioclase and quartz assemblages, this happens between 800 and  $900^\circ\text{C}$  at 1, 1.5, and 2 GPa. With small amounts of water added, melting starts below  $800^\circ\text{C}$  [Gardien *et al.*, 2000].

[49] We use the area with the highest heat flow in the THO, which lies near the city of Thompson in the belt of the same name. North of the Pipe Mine site, six independent sites (Birchtree Mine 1, Owl, Thompson, Mystery Lake, Bible Camp and Moak Lake) have a mean heat flow of  $53 \text{ mW m}^{-2}$  and the mean heat production of the metasediments is  $1.0 \mu\text{W m}^{-3}$ . Given their present average radioelement concentration (U = 1.07 ppm, Th = 8.18 ppm, K = 2.01%) and the decay constants of the relevant radioactive isotopes ( $^{40}\text{K}$ ,  $^{232}\text{Th}$ ,  $^{235}\text{U}$ , and  $^{238}\text{U}$ ), the average heat production of these rocks was 1.5 times higher 1.8 Ga ago than today. At the surface, these metasediments contain water-bearing minerals such as biotite and hornblende [Bleeker, 1990] and hence have not undergone dehydration melting. This is consistent with their “undepleted” radioelement concentrations, as any melting reaction would have led to both a dehydrated and depleted residue. These rocks would not be stable above a critical threshold temperature of about  $800^\circ\text{C}$ , or 1073 K. Lower crustal assemblages are not well-known, but would have higher solidus temperatures if they have no water-bearing minerals.

### 6.2. Thermal Model

[50] Few thermal conductivity measurements have been made in the 700–1200 K range of relevance to the lower

continental crust. The most extensive study available is by *Durham et al.* [1987] who have determined thermal diffusivity of many different types of igneous rocks at temperatures and pressures of up to 700 K and 200 MPa, respectively. In such conditions, heat transport is effected by lattice conduction (phonon transport). A best fit to all the data at room pressure leads to an empirical equation:

$$\alpha = 0.47 + 78T^{-1} - 1.31Q + 1540QT^{-1}, \quad (2)$$

where  $T$  is temperature in kelvins,  $\alpha$  is thermal diffusivity in  $\text{mm}^2/\text{s}$  and  $Q$  the volume fraction of quartz in the rock. The pressure effect is small in the range of relevance to crustal studies and can be ignored with little error. The average conductivity of Thompson belt rocks is  $3.1 \text{ W m}^{-1} \text{ K}^{-1}$  at room temperature, and we have used the Durham empirical equation with appropriate values for  $Q$ , density and thermal capacity. Rocks from granulite facies terrains have thermal conductivity values between  $3.0$  and  $3.5 \text{ W m}^{-1} \text{ K}^{-1}$  at room temperature [*Jöeleht and Kukkonen*, 1998]. Thus the same conductivity equation can be used throughout the crust.

[51] At temperatures larger than about 700–800 K, radiative heat transport becomes significant and leads to a conductivity increase [*Roy et al.*, 1981; *Clauser and Huenges*, 1995]. Laboratory data are available on mantle minerals at temperatures above 1000 K [*Schatz and Simmons*, 1972; *Schärmeli*, 1979; *Roy et al.*, 1981]. Radiative conductivity obeys the following law:

$$k = cT^3, \quad (3)$$

with coefficient  $c$  equal to about  $0.37 \times 10^{-9}$  in S.I. units [*Schatz and Simmons*, 1972; *Schärmeli*, 1979]. In our calculations, conductivity is taken as the sum of a lattice component which follows the Durham equation (2) and a radiation component which follows equation (3).

[52] Sample calculations are carried out to evaluate the effect of temperature-dependent conductivity and enhanced radiogenic heat production in the past. For the Thompson area, we assume a surface heat flow of  $53 \text{ mW m}^{-2}$  a mantle heat flow of  $15 \text{ mW m}^{-2}$ , corresponding to a total crustal contribution of  $38 \text{ mW m}^{-2}$ . The Moho discontinuity is not well identified in this area, implying that it is not a distinct reflector or that it is deeper than 50 km, the depth of investigation. In other parts of the Thompson belt, crustal thickness is  $\sim 48 \text{ km}$  [*Nemeth et al.*, 1996; *Nemeth and Hajnal*, 1997; *White et al.*, 1999]. Here, we shall take a crustal thickness of 48 km, implying a value of  $0.79 \mu\text{W m}^{-3}$  for the average crustal heat production. At 1.8 Ga, this heat production was  $1.2 \mu\text{W m}^{-3}$ . We further assume that radioelements are uniformly distributed throughout the crust. A conservative assumption is that the mantle heat flow was the same as today. Geotherms are shown in Figure 11. For comparison, we have used a constant conductivity of  $2.5 \text{ W m}^{-1} \text{ K}^{-1}$ , which is commonly used for thermal models of continental crust and which is close to the average value for the temperature-dependent conductivity. Temperatures in the Proterozoic are markedly higher than those prevailing today, and even higher with temperature-dependent conductivity. These estimates must be regarded as lower bounds for several reasons. In the past, the mantle heat flow was

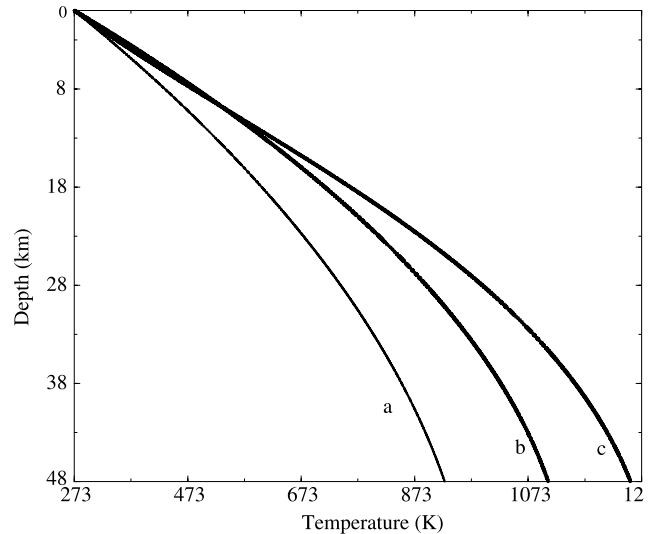


**Figure 11.** Crustal geotherms for the Thompson area and for a mantle heat flow of  $15 \text{ mW m}^{-2}$ . Curve a, today for a constant conductivity of  $2.5 \text{ W m}^{-1} \text{ K}^{-1}$ ; curve b, at 1.8 Ga, for the same constant conductivity value; curve c, at 1.8 Ga, for temperature-dependent conductivity.

probably higher than today. Furthermore, the Thompson belt has been eroded and the present-day crustal column used to lie at a depth of several kilometers. The calculations thus predict that temperatures in the Proterozoic were above the solidus over most of the lower crust. This is not consistent with the geological record which does not indicate late stage anatectic melting in the THO, implying that the starting model must be modified.

### 6.3. Deep Crustal Structure Beneath Thompson

[53] Throughout the following, we use temperature-dependent conductivity. In the Thompson area, the surface values of both heat flow and heat production are known, as well as the total crustal thickness. Thus temperature estimates rely on two inputs: the mantle heat flow value and the vertical distribution of heat production. The calculations of Figure 11 do not account for depletion in the lower crust. In the Thompson area, the surficial metasedimentary formations have a thickness of  $\sim 6 \text{ km}$  [*White et al.*, 1999]. Geological constraints indicate that these rocks overlie Archean crust of the Superior craton, which is well-known over a large depth extent thanks to exposures in the adjacent Pikwitonei-Sachigo area [*Fountain and Salisbury*, 1981]. Amphibolite-facies rocks of the Sachigo province have a mean heat production of  $1.0 \mu\text{W m}^{-3}$  [*Fountain et al.*, 1987], close to the average value for the Thompson belt supracrustals (Table 4). Granulite-facies rocks of the Pikwitonei province have a much lower average heat production of  $0.4 \mu\text{W m}^{-3}$  [*Fountain et al.*, 1987]. *White et al.* [1999] propose that at Thompson, the whole crustal column below the metasediments is made of Pikwitonei granulites. This yields a total crustal heat production about  $23 \text{ mW m}^{-2}$  and a mantle heat flow of  $30 \text{ mW m}^{-2}$ . This is higher than measured heat flow values at several locations in the THO, which is impossible. Thompson basement cannot be made exclusively of Pikwitonei granulites and probably includes a

thick section of Superior province crust including some amphibolite-facies rocks.

[54] In order to obtain crustal temperature estimates, with a given value of heat flow at the Moho, the only unknown is the vertical distribution of heat production. We shall use a two layer model because the difference with more complicated models is  $<50$  K, which is within the range of uncertainty of the model results. The great advantage of a two-layer model is that, for given mantle heat flow, there is only one unknown: the thickness or heat production of the lower crust.

[55] Recent studies have summarized current knowledge on heat production in deep continental crustal levels [Rudnick and Fountain, 1995; Jöeleht and Kukkonen, 1998]. Large data sets have been acquired in the Canadian Shield [Shaw *et al.*, 1994], the Baltic Shield [Jöeleht and Kukkonen, 1998] and the Indian Shield [Roy and Rao, 2000]. The lowermost crust cannot be sampled directly, except perhaps in the Ivrea Zone, Italy, and it is difficult to determine a reliable average heat production over the large scale required for heat flow studies [Jaupart, 1983]. Experimental studies show that chemical changes due to granulitic metamorphic reactions have only a weak influence on the two main heat-producing elements, uranium and thorium [Bingen *et al.*, 1996; Bea and Montero, 1999]. Therefore U and Th contents of lower crustal rocks are not determined by pressure and temperature conditions and only depend on prior magmatic history. Indeed, in the Baltic Shield, granulite facies terranes which have undergone different metamorphic evolutions have similar values of heat production [Jöeleht and Kukkonen, 1998]. It is worth recalling that many sampled areas are in the Canadian Shield or were part of the same landmass in the Precambrian (the Norwegian and Baltic Shield), and hence are directly relevant to the present study.

[56] Two different estimates of lower crustal heat production have been proposed using granulite facies terranes and xenoliths brought by basaltic magmas. Granulite facies terranes allow the sampling of large volumes of crustal material and the determination of a proper average with each rock type weighted according to its abundance. For depths of 15–30 km, a wide range of heat production values, from  $0.57$  to  $2.24 \mu\text{W m}^{-3}$ , are reported [Jöeleht and Kukkonen, 1998]. For the deepest samples buried at pressures of 8–11 kbar, representative of basal crustal conditions, the mean heat production is  $0.57 \mu\text{W m}^{-3}$ . Xenoliths have the advantage that they do come from *in situ* lower crust but it is debatable that they represent a random sample of all lithologies present at depth. Kimberlite pipes and basaltic dykes are limited to specific areas of a geological province. The sampling is biased by the geological process responsible for the ascent of basaltic magmas through the crust. Such ascent is buoyancy-driven, implying that basaltic magmas are not able to rise through rocks of lower density, *i.e.*, of felsic composition, and hence undersample evolved rocks with enriched compositions. Xenolith model compositions in Rudnick and Fountain [1995] are indeed systematically more mafic and depleted in radioelements than estimates from terrain exposures. Moreover, Uranium and Thorium exhibit highly skewed distributions which are poorly defined by the rather small number of measurements available. The median values are

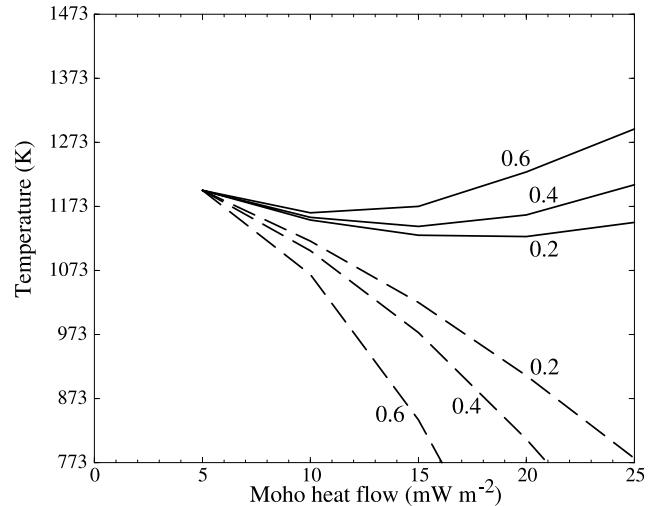


**Figure 12.** Moho temperature (solid lines) and temperature at the base of the upper crustal layer (dashed lines) in the Thompson crust 1.8 Ga ago. Calculations are made with a two-layer crustal model with different values of lower crustal heat production (shown along the curves in  $\mu\text{W m}^{-3}$ ).

systematically lower than the mean values, and Rudnick and Fountain chose the former. The resulting average heat production for the lower crust of  $0.18 \mu\text{W m}^{-3}$  should be regarded as a lower bound. In the following, we consider values for the lower crust in the range of  $0.2$ – $0.6 \mu\text{W m}^{-3}$ .

#### 6.4. Lower Bound on Mantle Heat Flow

[57] We shall now demonstrate that the condition that undepleted upper crustal rocks must remain below the melting temperature leads to a lower bound on the mantle heat flow. We consider a two-layer model for the Thompson crust. For the measured heat flow value of  $53 \text{ mW m}^{-2}$ , the total amount of heat generated in the crust is calculated as a function of the mantle heat flow. We fix the value of heat production in the upper crustal layer at  $1.0 \mu\text{W m}^{-3}$ , consistent with our surface measurements. For the Proterozoic (1.8 Ga), the crustal heat production is obtained by running backwards the decay reactions and the mantle heat flow is assumed to remain constant through time.

[58] As expected, for a given value of mantle heat flow, the two-layer crustal model leads to lower Moho temperatures than the homogeneous model. Predicted Moho temperatures increase with lower crustal heat production, because the crustal structure gets closer to the homogeneous model. In all cases, the Moho temperature is significantly above the threshold value for melting (1073 K). We have also calculated the temperature at the base of the upper layer as a function of mantle heat flow (Figure 12). This temperature decreases with increasing mantle heat flow, because the thickness of the layer decreases. As the lower crustal heat production is decreased, this temperature estimate increases because the upper layer must be made thicker. For values of lower crustal heat production lower than  $0.4 \mu\text{W m}^{-3}$  and mantle heat flow values lower than  $11 \text{ mW m}^{-2}$ , the base of the upper crust and the whole lower crust are above 1073 K, our postulated threshold melting temper-

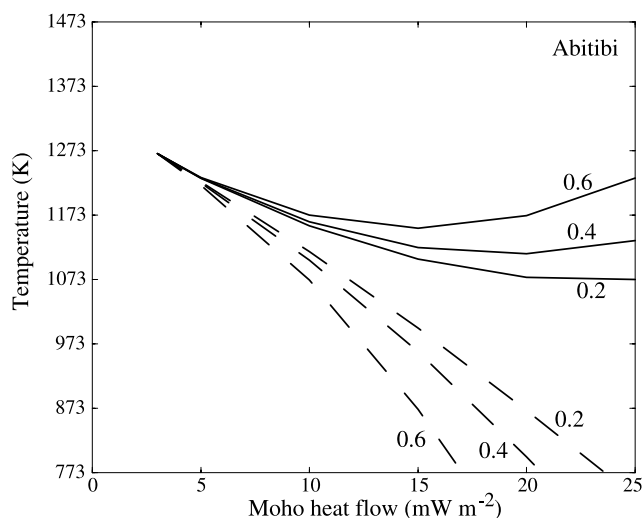


**Figure 13.** Moho temperature (solid lines) and temperature at the base of the upper crustal layer (dashed lines) in western Abitibi as a function of mantle heat flow at 2.7 Ga. The numbers along the curves refer to lower crustal heat production (in  $\mu\text{W m}^{-3}$ ).

ature. This provides a lower bound on the mantle heat flow value. This lower bound changes to  $12 \text{ mW m}^{-2}$  if the lower crustal heat production is  $0.2 \mu\text{W m}^{-3}$  (Figure 12).

[59] In reality, the crust is heterogeneous on a scale of  $\sim 10 \text{ km}$ , such that evolved and radiogenic units are found down to the Moho [Fountain and Salisbury, 1981]. Fluctuations depending on local heat production anomalies must be added to the 1-D temperature estimates. These horizontal fluctuations may be as large as  $50 \text{ K}$ , close to uncertainties associated with the vertical heat production profile. Thus, by requiring that melting temperatures are not reached in a 1-D model, we err on the conservative side.

### 6.5. Archean Abitibi Subprovince

[60] We can use the same line of argument for other geological provinces. In order to emphasize the effects of age, we have chosen an area in the Abitibi subprovince, a well-known part of the Archean Superior Province [Pinet et al., 1991; Guillou et al., 1994]. In western Abitibi, the surface heat flow reaches a local average value of  $52 \text{ mW m}^{-2}$  [Jaupart and Mareschal, 1999]. There, the crustal thickness is  $41 \text{ km}$ , the upper crust consists of tonalites with a mean heat production of  $1.2 \mu\text{W m}^{-3}$  [Green et al., 1990; Pinet et al., 1991; Guillou et al., 1994; Mareschal et al., 2000a]. Midcrustal material in the Abitibi is made of granulite terranes which have been brought to the surface by low-angle thrusts in the Kapuskasing zone [Percival et al., 1989]. Comprehensive surface sampling allows a reliable estimate of midcrustal heat production of  $0.5 \mu\text{W m}^{-3}$  [Shaw et al., 1994].

[61] We use the same procedure as before to investigate thermal conditions in the Abitibi crust. The last thermal event to affect the Abitibi dates from  $2.7 \text{ Ga}$ . At that time, heat production was higher than today by a factor of  $2.0$ . Using a two-layer crustal model, and setting the lower crustal heat production at the value of  $0.2 \mu\text{W m}^{-3}$ , we obtain a lower bound of  $12 \text{ mW m}^{-2}$  for the mantle heat

flow (Figure 13). Coincidentally, this result is identical to the one obtained for the Thompson crustal block in the Proterozoic. The greater age of the Abitibi compensates for its somewhat thinner crust.

## 7. Discussion and Conclusion

[62] New heat flow and heat production data in the Trans-Hudson Orogen provide constraints on crustal structure. The average heat flow for the THO, based on 45 determinations, is  $42 \pm 1.4 \text{ mW m}^{-2}$ , which is identical to the values reported by Mareschal et al. [1999a]. The large standard deviation of heat flow ( $9 \text{ mW m}^{-2}$ ) reflects important variations of bulk crustal composition and heat production. Such variations may be assessed in several regions where geological and geophysical models are consistent with heat flow data. Low heat flow regions provide an upper bound for the mantle heat flow. In high heat flow areas of the THO, crustal rocks are at high temperatures today and were still hotter in the past due to higher radiogenic heat production. The condition of thermal stability provides a lower bound on the mantle heat flow. Combining the two independent bounds, we arrive at a range of  $11\text{--}16 \text{ mW m}^{-2}$  for the mantle heat flow beneath the THO. This is not significantly different from the values obtained by Guillou-Frottier et al. [1995] in the Abitibi using completely different arguments. Petrological data on mantle xenoliths have led to similar estimates of the mantle heat flow beneath the Canadian and Fennoscandian shields [Jokinen and Kukkonen, 1999; Russell and Kopylova, 1999].

[63] The mantle heat flow value has implications for the thermal structure of continental crust and the thickness of continental lithosphere. Using a variety of constraints and allowing for uncertainties in parameter values and model assumptions, Jaupart and Mareschal [1999] concluded that lithosphere thickness beneath old cratons is unlikely to be smaller than  $200 \text{ km}$  and larger than  $350 \text{ km}$ . Using a small-scale convection model for heat transport into the lithosphere, Jaupart et al. [1998] proposed a more restricted range of  $200\text{--}250 \text{ km}$ . The values obtained for the THO are consistent with these earlier estimates. Thus heat flow data provide no evidence for major differences of heat supply into the lithosphere throughout the Precambrian Shield of North America.

[64] With a uniform mantle heat flow value, Moho temperatures vary between belts of the THO because of differences in crustal heat production. Present-day Moho temperatures are estimated to be as low as  $300^\circ\text{C}$  beneath Lynn Lake area and as high as  $600^\circ\text{C}$  beneath Thompson. Such large variations of crustal temperatures have significant implications for mechanical behavior and for thermal stability. They occur on horizontal scales of  $\sim 300 \text{ km}$  and are smoothed out by horizontal conduction below the Moho. Thus they do not lead to significant thermal differences at the base of the lithosphere if it is deeper than  $200 \text{ km}$ .

## Appendix A: Other Data

### A1. Flin Flon-Snow Lake Belt

[65] In three boreholes at the Leo Lake site (9806, 9807, and 9909), temperature logs yield a stable gradient of  $\sim 11 \text{ mK m}^{-1}$  (Table A1) close to those measured elsewhere in the Flin Flon belt. However, these wells are located within a

**Table A1.** Other Data

Site Hole	Lat North	Long West	Dip, deg	$\Delta h$ , m	$N_k$	$\langle k \rangle$ , $W m^{-1} K^{-1}$	$G$ , mK $m^{-1}$
<i>Flin Flon-Snow Lake Belt</i>							
Leo Lake							
98-06	54 47 24	101 34 11	59	268–477	11	5.51	11.2
98-07	54 47 24	101 34 12	52	198–440	10	5.94	10.9
99-09	54 47 25	101 34 19	64	237–596	13	5.11	10.7
<i>Athabasca Basin</i>							
Cluff Lake							
99-20	58 22 36	109 32 28	90	100–300	6	3.38	17.7
Shea Creek							
99-22	58 13 49	109 31 12	90	260–530	7	6.02	7.7
99-23	58 13 49	109 31 12	90	100–380	5	6.02	8.3

body with anomalously high thermal conductivity ( $5.5 W m^{-1} K^{-1}$ ), close to the boundary with mafic volcanics with lower conductivity ( $\sim 3.2 W m^{-1} K^{-1}$ ). In this case refraction effects must be taken into account (Appendix B).

## A2. Athabasca Basin

[66] The Athabasca Basin is located northwest of the exposed Trans-Hudson Orogen (Figure 1). Basement of the Rae-Hearne Province crops out to the north and the south of this basin and is exposed within the Carswell structure, a meteorite impact. We have measured two sites within and south of this structure, at Cluff Lake (hole 9920) and Shea Creek (holes 9922 and 9923).

[67] The Cluff Lake borehole is located near a uranium mine within the Carswell structure. There, an older granitoid complex is overlain by a supracrustal sequence of gneisses. In these altered gneisses, the temperature gradient is high ( $17.7 mK m^{-1}$ ) and unfortunately not stable. Using only the deepest section where thermal conductivity is  $3.38 W m^{-1} K^{-1}$ , we obtain a heat flow estimate of  $60 mW m^{-2}$  which is not reliable. To the north of this site, an older reliable heat flow determination of  $56 mW m^{-2}$  is available at the mining town of Eldorado [Jessop *et al.*, 1984].

[68] At Shea Creek, a few kilometers south of the Carswell structure, two boreholes go through hematized quartz sandstones and conglomerates of the Athabasca, deposited 1.7 to 1.6 Ga. At this site, the sediments are about 700 m thick and our measurements barely penetrate into the basement. Temperature gradients are low ( $8 mK m^{-1}$ ) and very perturbed (Figure A1), which can be attributed to ground-water circulation with certainty because the rocks are highly fractured and permeable. Using the high thermal conductivity of these quartz-rich sediments ( $6.02 W m^{-1} K^{-1}$ ), we obtain a heat flow estimate of  $48 mW m^{-2}$  for Shea Creek. This value is clearly uncertain, but is close to a value reported by Drury [1985] for the Rumpel Lake site located farther south in the Athabasca Basin ( $39 mW m^{-2}$ ).

[69] These two sites in the Athabasca basin cannot be considered reliable and hence we do not give heat flow determinations for them. However, they do not reveal heat flow anomalies and are consistent with previous measurements.

## Appendix B: Refraction Effects

[70] The THO has been severely deformed and folded, resulting in intricate successions of rocks with different origins, compositions and physical properties. At several

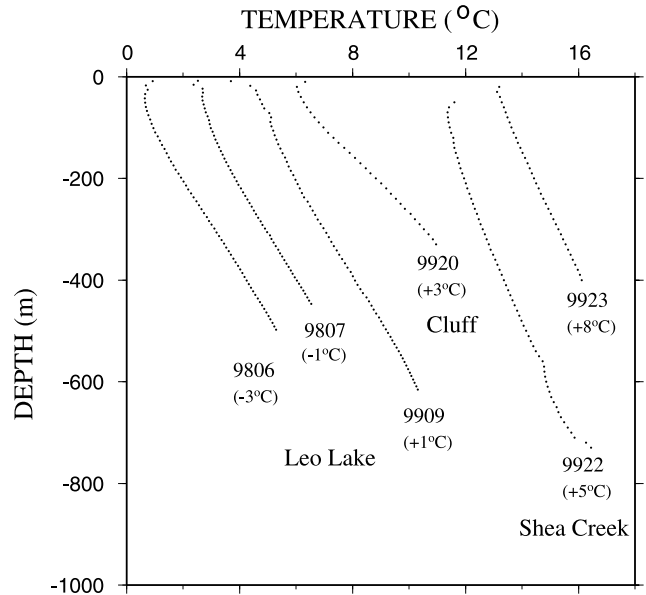


**Figure A1.** Temperature-depth profiles measured for Leo Lake, Cluff Lake and Shea Creek sites. The temperature profiles are shifted horizontally as indicated for clarity.

locations, large contrasts of thermal conductivity generate marked heat refraction effects which must be accounted for.

## B1. Loonhead Site

[71] The borehole drilled in felsic volcanic sequences intersects an intermediate volcanic intrusive with thermal conductivity smaller than in the felsic surroundings ( $2.6 W m^{-1} K^{-1}$  instead of  $3.9 W m^{-1} K^{-1}$ ). The two sharply discontinuities observed in the heat flow profile (left part of Figure B1) are characteristic of local heat refraction effects.

[72] A geological cross section around the borehole indicates an inclined,  $\sim 100 m$  thick layer of intermediate volcanics which cut the borehole at depth of  $\sim 350 m$ . We model an inclined lower conductivity layer in more conductive surroundings. A constant heat flow of  $10 mW m^{-2}$

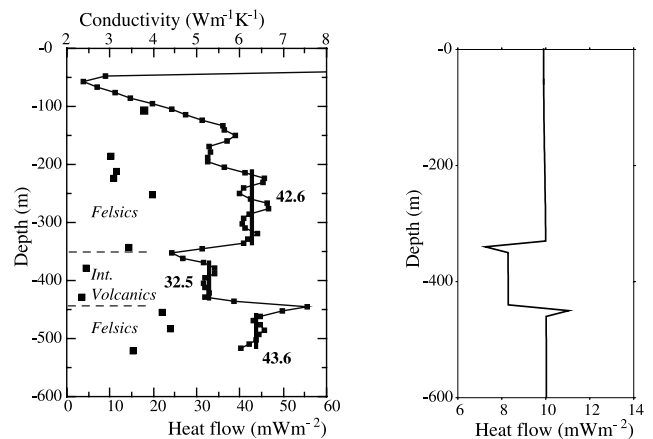


**Figure B1.** Measured (left) and modeled (right) heat flow profiles for the Loonhead site. Conductivity measurements are shown by squares. For the model, the conductivity of the volcanics is  $2.6 W m^{-1} K^{-1}$  versus  $3.9 W m^{-1} K^{-1}$  for the felsic rocks.

is imposed at depth, a constant temperature at the surface and we solve for the 2-D steady state heat equation with a finite element code. The predicted heat flow distribution is shown in the right part of Figure B1 for a conductivity contrast of 1.5, appropriate for the Loonhead borehole. *Hyndman and Sass* [1966] have proposed an approximate correction procedure for heat refraction at a sloping interface between media of different thermal conductivity. Our exact numerical calculation shows the disturbed shape of the heat flow profile within and away from a thin sloping layer. This model perfectly reproduces the measured heat flow profile and indicates that the undisturbed heat flow value may be safely determined at small distances from the low conductivity horizon.

## B2. Leo Lake Site

[73] The local heat flow at the Leo Lake sites is high,  $65 \text{ mW m}^{-2}$ , in a massive body ( $\sim 5 \text{ km} \times 5 \text{ km}$ ) of highly conductive metamorphosed felsic volcanics. It is not possible to correct these measurements for heat refraction because we have no information on the size and shape of the conducting body at depth. However, we may estimate the magnitude of the refraction effect using simple theoretical models [*Guillou-Frottier et al.*, 1996]. We take a cylindrical conductor which is embedded in a half-space. For the conductivity contrast of 1.6 appropriate for this site, we find that, depending on the aspect ratio of the conductor, heat flow may be increased by as much as 1.7 near the boundary. The corrected heat flow value may therefore be as small as  $39 \text{ mW m}^{-2}$ , which is close to other measurements in the area. Although the Leo Lake site does not provide a reliable heat flow determination, it is clearly not anomalous with respect to the Flin Flon belt.

## B3. Thompson Belt

[74] Two anomalously high heat flow values are recorded in high-conductivity quartz-rich metasediments in the northern part of the Thompson belt [*Guillou-Frottier et al.*, 1996] (Figure 10). At the “Birchtree Mine” site, we have measured two deep boreholes 3 km apart with heat flow values of 50 and  $64 \text{ mW m}^{-2}$ . The smallest value is recorded through a massive gneiss body with “normal” conductivity values and the highest value through a quartz-rich lens. At the northern site called “Thompson Train Station”, three individual determinations are available in deep boreholes. Two large heat flow values of  $81 \text{ mW m}^{-2}$  are recorded through a massive quartzite lens, and a lower value of  $59 \text{ mW m}^{-2}$  is obtained in “normal” metasediments at a distance of  $\sim 3 \text{ km}$ .

[75] In both cases, the anomalous bodies are deep ( $>1.5 \text{ km}$ ) and subvertical with elliptical horizontal cross sections, and are interpreted as sheath folds which were turned upright during the Hudsonian orogeny [*Bleeker*, 1990]. They are lined up with thin ( $\sim 100 \text{ m}$ ) high-conductivity veneers where the heat flow boreholes are located. Locally, one may approximate these structures by a thin vertical sheet embedded in a half-space. Our calculations show that heat refraction effects are limited to the conducting sheet, with no detectable heat flow perturbations in the surrounding rocks. The physical reason for this is as follows. The refraction effect occurs on a horizontal scale which is close to the vertical extent of the sheet. The temperature field is continuous and, close to the upper boundary where temper-

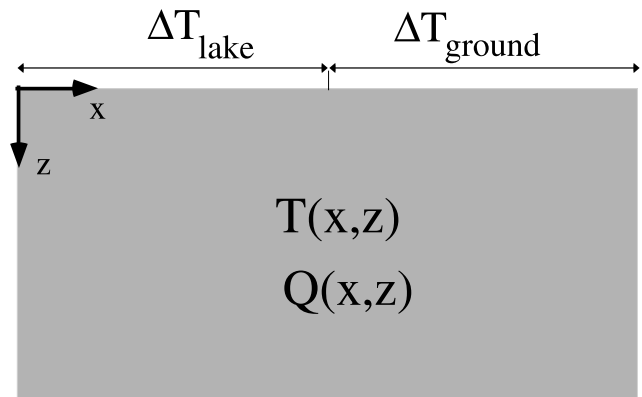


**Figure C1.** Surface boundary conditions to evaluate shallow heat flow perturbations due to recent warming in the vicinity of a lake.

ature is uniform, there are only very small lateral temperature variations. Thus the surface heat flow pattern is an anomalously high value over the sheet, compensated by heat flow values lower than normal in the surroundings. The latter are spread over a large horizontal distance and hence it takes a tiny reduction to compensate for the local high in the thin sheet. In practice, one may obtain unperturbed heat flow values at distances of  $<100 \text{ m}$  from the conducting sheet. Thus we exclude the very high heat flow values at the “Birchtree Mine” and “Thompson Train Station” sites and retain the heat flow values obtained through rocks with “normal” conductivity values.

## B4. Overview

[76] There are several instances of marked heat refraction effects in the THO, and one may wonder whether such perturbations may have gone unnoticed at other locations. The most dramatic effects are observed through vertical inclusions, and close to the boundary between two bodies with large contrasts of thermal properties. In all cases but one (Leo Lake) the conducting bodies are thin ( $\sim 100 \text{ m}$  wide) and heat flow perturbations decay over a few tens of meters, as shown by data and calculations for the Loonhead site (Figure B1). A clear fingerprint of heat refraction is a correlation between heat flow and thermal conductivity. Examination of the data in the various belts of the THO shows no such correlation. For example, in the southern volcanic belt, the lowest heat flow at Morgan Lake ( $28 \text{ mW m}^{-2}$ ) is obtained through rocks with higher conductivity than those at Chisel Lake 20 km away, where heat flow is higher (Table 1).

[77] We have multiplied the measurements in order to ascertain the properties of the various rocks in the THO and to identify the anomalous sites. Ten boreholes, within an area  $\sim 400 \text{ m} \times 500 \text{ m}$ , were logged at the Pipe Mine site in the Thompson belt in order to study recent ground surface temperature variations. For the 10 profiles, the temperature gradients at 300 m depth are almost identical ( $15.5 \pm 0.2 \text{ mK m}^{-1}$ ). This shows that there is no refraction effect over a few hundred meters.

## Appendix C: Climatic Correction

[78] Elevated ground surface temperatures are observed for three sites located on lake shores, Suggi Lake, Morgan

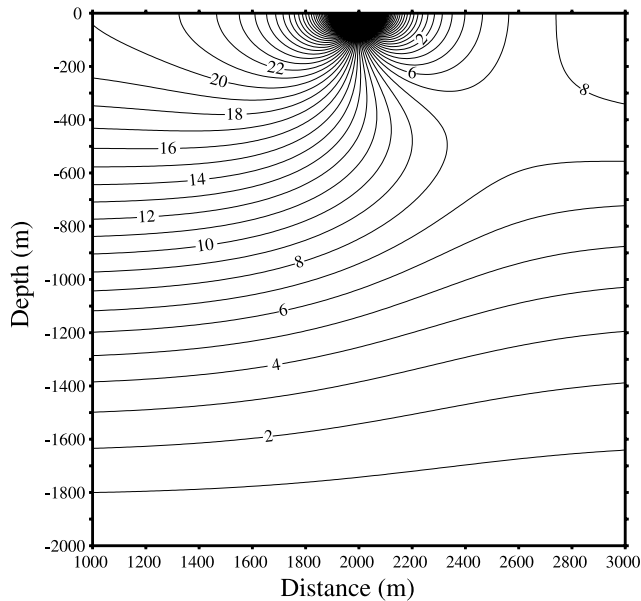


**Figure C2.** Contours of heat flow perturbations due to differential warming near a lake shore. Contours are shown with increments of  $1 \text{ mW m}^{-2}$ . A zero basal heat flow is imposed at depth. Surface temperature was initially  $-1^\circ\text{C}$  everywhere beneath the ice sheet and was set to  $5.5^\circ\text{C}$  beneath the lake (left-hand side) and to  $2^\circ\text{C}$  on dry land (right-hand side), when the ice sheet melted 10,000 years ago. The lake shore lies in the middle of the figure, at the 2000 m distance mark.

Lake, and Mystic Lake. In these three sites, the same features are observed over the topmost few hundred meters. The temperature gradient and the heat flow decrease with depth. Therefore the temperatures at shallow depth are lower than those obtained by upward continuation of the deepest part of the profile. This feature can be accounted for by horizontal heat conduction due to differences in ground temperatures between the lake and dry land. In the THO, yearly average ground temperatures on dry land vary between  $3^\circ\text{C}$  near Flin Flon and  $1^\circ\text{C}$  near Lynn Lake. Measurements made in many lakes in Manitoba and neighboring Ontario show yearly average bottom-lake temperatures at the top of the sediments between  $3.5^\circ\text{C}$  and  $6.5^\circ\text{C}$  [Allis and Garland, 1979]. This shows that temperatures are higher beneath a lake than on dry land. In this case, the standard procedure for climatic correction is inappropriate as it assumes uniform ground temperature warming when the ice sheet melted away.

[79] At the Suggi Lake, Morgan Lake, and Mystic Lake sites, the boreholes are not vertical and dip toward the lake, with their deepest section well away from the shore. The contrast between lake and dry land dates from the deglaciation, about 10,000 years ago in the THO. Over this time, heat diffusion affects temperatures over a distance of about 700 m. We have carried out a transient 2-D calculation to investigate the temperature field near a lake shore (Figure C1). Following the standard correction model of Jessop [1971], we assume that the surface temperature was  $-1^\circ\text{C}$  everywhere during the last glacial period and that at 10 ky before present it jumped to  $5.5^\circ\text{C}$  beneath the lake and  $2^\circ\text{C}$

on dry land. We find that, deeper than about 300 m and at distances from the lake shore larger than  $\sim 300$  m, temperatures are close to those of a 1-D thermal model for vertical heat transport (Figure C2). In other words, it is appropriate to make the correction in the deep sections of our boreholes as if the surface temperature had been set to the lake bottom value. The recent post-glacial warming is only the last one in a series of climatic changes and the full correction procedure accounts for those as well [Jessop, 1971].

[80] For the three lake shore sites, we therefore proceed as follows. The lake bottom temperature is determined by extrapolating the deepest part of the vertical temperature profile toward the surface. We obtain the following values:  $6.2^\circ\text{C}$  at Suggi Lake,  $5.5^\circ\text{C}$  at Morgan Lake, and  $4.6^\circ\text{C}$  at Mystic Lake. The correction is small and even a large error on the correction has a small impact on the final heat flow value.

[81] **Acknowledgments.** The authors are grateful to the many geologists in mining and exploration companies for their help in the field. David Blackwell, an anonymous reviewer, and Associate Editor Adrian Lenardic are thanked for critical reviews and useful comments which helped in improving the manuscript. This research was supported by INSU (CNRS, France), NSERC (Canada), and FCAR (Québec). This is LITHOPROBE publication 1278.

## References

- Allis, R. G., and G. D. Garland, Heat flow measurements under some lakes in the Superior Province of the Canadian Shield, *Can. J. Earth Sci.*, **16**, 1951–1964, 1979.
- Ashton, K. E., L. M. Heaman, J. F. Lewry, R. P. Hartlaub, and R. Shi, Age and origin of the Jan Lake Complex: A glimpse at the buried Archean craton of the Trans-Hudson Orogen, *Can. J. Earth Sci.*, **36**, 185–208, 1999.
- Ashwal, L. D., P. Morgan, S. A. Kelley, and J. Percival, Heat production in an Archean crustal profile and implications for heat flow and mobilization of heat producing elements, *Earth Planet. Sci. Lett.*, **85**, 439–450, 1987.
- Baldwin, D. A., E. C. Syme, H. V. Zwanzig, T. M. Gordon, P. A. Hunt, and R. D. Stevens, U-Pb zircon ages from the Lynn Lake and Rusty Lake metavolcanic belts, Manitoba: Two ages of Proterozoic magmatism, *Can. J. Earth Sci.*, **24**, 1053–1063, 1987.
- Bea, F., and P. Montero, Behavior of accessory phases and redistribution of Zr, REE, Y, Th, and U during metamorphism and partial melting of metapelites in the lower crust: An example from the Kinzigite Formation of Ivrea-Verbano, NW Italy, *Geochim. Cosmochim. Acta*, **63**, 1133–1153, 1999.
- Bingen, B., D. Demaiffe, and J. Hertogen, Redistribution of rare earth elements, thorium, and uranium over accessory minerals in the course of amphibolite to granulite facies metamorphism: The role of apatite and monazite in orthogneisses from southwestern Norway, *Geochim. Cosmochim. Acta*, **60**, 1341–1354, 1996.
- Birch, F., E. R. Roy, and E. R. Decker, Heat flow and thermal history in New England and New York, in *Studies of Appalachian Geology*, edited by E. An-Zen, pp. 437–451, Wiley-Interscience, New York, 1968.
- Blackwell, D. D., J. L. Steele, S. Kelley, and M. A. Korosec, Heat flow in the state of Washington and thermal conditions in the Cascade range, *J. Geophys. Res.*, **95**, 19,495–19,516, 1990.
- Bleeker, W., New structural-metamorphic constraints on Early Proterozoic oblique collision along the Thompson Nickel Belt, Manitoba, Canada, in *The Early Proterozoic Trans-Hudson Orogen of North America*, edited by J. F. Lewry and M. R. Stauffer, *Geol. Assoc. Can. Spec. Pap.*, **37**, 57–73, 1990.
- Burwash, R. A., and G. L. Cumming, Uranium and thorium in the Precambrian basement of western Canada, I, Abundance and distribution, *Can. J. Earth Sci.*, **13**, 284–293, 1976.
- Clauser, C. and E. Huenges, Thermal conductivity of rocks and minerals, in *Rock Physics and Phase Relations: A Handbook of Physical Constants*, edited by T. J. Ahrens, AGU, Washington, D. C., 1995.
- Clemens, J. D., and D. Vielzeuf, Constraints on melting and magma production in the crust, *Earth Planet. Sci. Lett.*, **86**, 287–306, 1987.
- Decker, E. R., K. R. Baker, G. J. Bucher, and H. P. Heasler, Preliminary heat flow and radioactive studies in Wyoming, *J. Geophys. Res.*, **85**, 311–321, 1980.

- Drury, M. J., Heat flow and heat generation in the Churchill Province of the Canadian Shield, and their paleotectonic significance, *Tectonophysics*, 115, 25–44, 1985.
- Durham, W. B., V. V. Mirkovich, and H. C. Heard, Thermal diffusivity of igneous rocks at elevated pressure and temperature, *J. Geophys. Res.*, 92, 11,615–11,634, 1987.
- England, P. C., E. R. Oxburg, and S. W. Richardson, Heat refraction in and around granites in north-east England, *Geophys. J. R. Astron. Soc.*, 62, 439–455, 1980.
- Ferguson, I. J., A. G. Jones, Y. Sheng, X. Wu, and I. Shiozaki, Geoelectric response and crustal electrical-conductivity structure of the Flin Flon Belt, Trans-Hudson Orogen, Canada, *Can. J. Earth Sci.*, 36, 1917–1938, 1999.
- Fountain, D. M., and M. H. Salisbury, Exposed cross-sections of the continental crust: Implications for crustal structure petrology, and evolution, *Earth Planet. Sci. Lett.*, 56, 263–277, 1981.
- Fountain, D. M., M. H. Salisbury, and K. P. Furlong, Heat production and thermal conductivity of rocks from the Pikwitonei-Sachigo continental cross section, central Manitoba: Implications for the thermal structure of Archean crust, *Can. J. Earth Sci.*, 24, 1583–1594, 1987.
- Gardien, V., A. B. Thompson, and P. Ulmer, Melting of biotite + plagioclase + quartz gneisses: The role of H<sub>2</sub>O in the stability of amphibole, *J. Petrol.*, 41, 651–666, 2000.
- Green, A. G., B. Milkereit, L. J. Mayrand, J. N. Ludden, C. Hubert, S. L. Jackson, R. H. Sutcliffe, G. F. West, P. Verpaalst, and A. Simard, Deep structure of an Archean greenstone terrane, *Nature*, 344, 327–330, 1990.
- Guillou, L., J. C. Mareschal, C. Jaupart, C. Gariépy, G. Bienfait, and R. Lapointe, Heat flow gravity and structure of the Abitibi belt, Superior Province, Canada: Implications for mantle heat flow, *Earth Planet. Sci. Lett.*, 122, 103–123, 1994.
- Guillou-Frottier, L., J.-C. Mareschal, C. Jaupart, C. Gariépy, R. Lapointe, and G. Bienfait, Heat flow variations in the Grenville Province, Canada, *Earth Planet. Sci. Lett.*, 136, 447–460, 1995.
- Guillou-Frottier, L., C. Jaupart, J. C. Mareschal, C. Gariépy, G. Bienfait, L. Z. Cheng, and R. Lapointe, High heat flow in the Thompson belt of the Trans-Hudson Orogen, Canadian Shield, *Geophys. Res. Lett.*, 23, 3027–3030, 1996.
- Hajnal, Z., S. B. Lucas, D. J. White, J. Lewry, S. Bezdán, M. R. Stauffer, and M. D. Thomas, Seismic reflection images of strike-slip faults and linked detachments in the Trans-Hudson Orogen, *Tectonophysics*, 15, 427–439, 1995.
- Hyndman, R. D., and J. H. Sass, Geothermal measurements at Mount Isa, Queensland, *J. Geophys. Res.*, 71, 587–601, 1966.
- Jaupart, C., Horizontal heat transfer due to radioactivity contrasts: Causes and consequences of the linear heat flow-heat production relationship, *Geophys. J. R. Astron. Soc.*, 75, 411–435, 1983.
- Jaupart, C., and J. C. Mareschal, The thermal structure of continental roots, *Lithos*, 48, 93–114, 1999.
- Jaupart, C., J. C. Mareschal, L. Guillou-Frottier, and A. Davaille, Heat flow and thickness of the lithosphere in the Canadian Shield, *J. Geophys. Res.*, 103, 15,269–15,286, 1998.
- Jessop, A. M., The distribution of glacial perturbation of heat flow in Canada, *Can. J. Earth Sci.*, 8, 162–166, 1971.
- Jessop, A. M., T. J. Lewis, A. S. Judge, A. E. Taylor, and M. J. Drury, Terrestrial heat flow in Canada, *Tectonophysics*, 103, 239–261, 1984.
- Jöeleht, A., and I. T. Kukkonen, Thermal properties of granulite facies rocks in the Precambrian basement of Finland and Estonia, *Tectonophysics*, 291, 195–203, 1998.
- Jokinen, J., and I. T. Kukkonen, Inverse simulation of the lithospheric thermal regime in the Fennoscandian shield using xenolith-derived mantle temperatures, *Tectonophysics*, 306, 293–310, 1999.
- Leclair, A. D., S. B. Lucas, H. J. Broome, D. W. Viljoen, and W. Weber, Regional mapping of Precambrian basement beneath Phanerozoic cover in southeastern Trans-Hudson Orogen, Manitoba and Saskatchewan, *Can. J. Earth Sci.*, 34, 618–634, 1997.
- Lewry, J. F., Z. Hajnal, A. Green, S. B. Lucas, D. J. White, M. R. Stauffer, K. E. Ashton, W. Weber, and R. Clowes, Structure of a Paleoproterozoic continent-continent collision zone: A Lithoprobe seismic reflection profile across the Trans-Hudson Orogen, Canada, *Tectonophysics*, 232, 143–160, 1994.
- Lucas, S. B., A. Green, Z. Hajnal, D. White, J. Lewry, K. Ashton, W. Weber, and R. Clowes, Deep seismic profile across a Proterozoic collision zone: Surprises at depth, *Nature*, 363, 339–342, 1993.
- Lucas, S. B., R. A. Stern, E. C. Syme, B. A. Reilly, and D. J. Thomas, Intraoceanic tectonics and the development of continental crust: 1.92–1.84 Ga evolution of the Flin Flon belt (Canada), *Geol. Soc. Am. Bull.*, 108, 602–629, 1996.
- Mareschal, J.-C., C. Pinet, C. Gariépy, C. Jaupart, G. Bienfait, G. Dalla-Coletta, J. Jolivet, and R. Lapointe, New heat flow density and radiogenic heat production data in the Canadian Shield and the Québec Appalachians, *Can. J. Earth Sci.*, 26, 845–852, 1989.
- Mareschal, J.-C., C. Jaupart, L.-Z. Cheng, F. Rolandone, C. Gariépy, G. Bienfait, L. Guillou-Frottier, and R. Lapointe, Heat flow in the Trans-Hudson Orogen of the Canadian Shield: Implications for Proterozoic continental growth, *J. Geophys. Res.*, 104, 29,007–29,024, 1999a.
- Mareschal, J. C., F. Rolandone, and G. Bienfait, Heat flow variations in a deep borehole near Sept-Îles, Québec, Canada: Paleoclimatic interpretation and implications for regional heat flow estimates, *Geophys. Res. Lett.*, 26, 2049–2052, 1999b.
- Mareschal, J.-C., C. Jaupart, C. Gariépy, L. Z. Cheng, L. Guillou-Frottier, G. Bienfait, and R. Lapointe, Heat flow and deep thermal structure near the edge of the Canadian Shield, *Can. J. Earth Sci.*, 37, 399–414, 2000a.
- Mareschal, J.-C., A. Poirier, F. Rolandone, G. Bienfait, C. Gariépy, R. Lapointe, and C. Jaupart, Low mantle heat flow at the edge of the North American continent, Voisey Bay, Labrador, *Geophys. Res. Lett.*, 27, 823–826, 2000b.
- Maxeiner, R. O., T. I. Sibbald, W. L. Slimmon, L. M. Heaman, and B. R. Watters, Lithogeochemistry of volcano-plutonic assemblages of the southern Hanson Lake Block and southeastern Glennie Domain, Trans-Hudson Orogen: Evidence for a single island arc complex, *Can. J. Earth Sci.*, 36, 209–225, 1999.
- Misener, A. D. and A. E. Beck, The measurement of heat flow over land, in *Methods and Techniques in Geophysics*, edited by S. K. Runcorn, pp. 10–61, Interscience, New York, 1960.
- Morgan, P., Crustal radiogenic heat production and the selective survival of continental crust, *J. Geophys. Res.*, 90, C561–C570, 1985.
- Nemeth, B., and Z. Hajnal, Structure of the lithospheric mantle beneath the Trans-Hudson Orogen, Canada, *Lithoprobe Rep.*, 62, 269–286, 1997.
- Nemeth, B., Z. Hajnal, and S. Lucas, Moho signature from wide angle reflections: Preliminary results of the 1993 Lithoprobe seismic refraction experiment, *Tectonophysics*, 264, 111–121, 1996.
- Nyblade, A. A., and H. N. Pollack, A global analysis of heat flow from Precambrian terrains: Implications for the thermal structure of Archean and Proterozoic lithosphere, *J. Geophys. Res.*, 98, 12,207–12,218, 1993.
- Pandit, B. I., Z. Hajnal, M. R. Stauffer, J. Lewry, and K. E. Ashton, New seismic images of the crust in the central Trans-Hudson Orogen of Saskatchewan, *Tectonophysics*, 290, 211–219, 1998.
- Patino Douce, E., and J. S. Beard, Dehydration-melting of biotite gneiss and quartz amphibolite from 3 to 15 kbar, *J. Petrol.*, 36, 707–738, 1995.
- Percival, J. A., A. G. Green, B. Milkereit, F. A. Cook, W. Geis, and G. F. West, Seismic reflection profiles across deep continental crust exposed in the Kapuskasing uplift structure, *Nature*, 342, 416–420, 1989.
- Pinet, C., C. Jaupart, J. C. Mareschal, C. Gariépy, G. Bienfait, and R. Lapointe, Heat flow and structure of the lithosphere in the eastern Canadian Shield, *J. Geophys. Res.*, 96, 19,941–19,963, 1991.
- Roy, R. F., A. E. Beck, and Y. S. Touloukian, Thermophysical properties of rocks, in *Physical Properties of Rocks and Minerals, McGraw-Hill CINDAS Data Ser. Mater. Prop.*, vol. 2, edited by Y. S. Touloukian, W. R. Judd, and R. F. Roy, pp. 409–502, McGraw-Hill, New York, 1981.
- Roy, S., and R. U. M. Rao, Heat flow in the Indian shield, *J. Geophys. Res.*, 105, 25,587–25,604, 2000.
- Rudnick, R. L., and D. M. Fountain, Nature and composition of the continental crust: A lower crustal perspective, *Rev. Geophys.*, 33, 267–309, 1995.
- Russell, J. K., and M. G. Kopylova, A steady-state conductive geotherm for the north central Slave, Canada: Inversion of petrological data from the Jericho Kimberlite pipe, *J. Geophys. Res.*, 104, 7089–7101, 1999.
- Sass, J. H., A. H. Lachenbruch, and A. M. Jessop, Uniform heat flow in a deep hole in the Canadian Shield and its paleoclimatic implications, *J. Geophys. Res.*, 76, 8586–8596, 1971.
- Schärmeli, G., Identification of radiative thermal conductivity in olivine up to 25 kbar and 1500K, in *Proceedings of 6th AIRAPT Conference*, edited by K. D. Timmerhauf and M. S. Barber, pp. 60–74, Plenum, New York, 1979.
- Schatz, J. F., and G. Simmons, Thermal conductivity of Earth materials, *J. Geophys. Res.*, 77, 6966–6983, 1972.
- Shaw, D. M., A. P. Dickin, H. Li, R. H. McNutt, H. P. Schwarcz, and M. G. Truscott, Crustal geochemistry in the Wawa-Foley region, Ontario, *Can. J. Earth Sci.*, 31, 1104–1121, 1994.
- Wang, Y., and J.-C. Mareschal, Elastic thickness of the lithosphere in the central Canadian Shield, *Geophys. Res. Lett.*, 26, 3033–3035, 1999.
- Wheeler, J. O., P. F. Hoffman, K. D. Card, A. Davidson, B. V. Sanford, A. G. Okulitch, and W. R. Roest, Geological map of Canada, *Map D1806A*, Nat. Resour. Can., Ottawa, Ont., 1997.
- White, D. J., A. G. Jones, S. B. Lucas, and Z. Hajnal, Tectonic evolution of the Superior Boundary zone from coincident seismic reflection and magnetotelluric profiles, *Tectonics*, 18, 430–451, 1999.

- White, D. J., H. V. Zwanzig, and Z. Hajnal, Crustal suture preserved in the Paleoproterozoic Trans-Hudson Orogen, Canada, *Geology*, 28, 527–530, 2000.
- Zelt, B. C., and R. M. Ellis, Receiver-function studies in the Trans-Hudson Orogen, Saskatchewan, *Can. J. Earth Sci.*, 36, 585–603, 1999.
- Zwanzig, H. V., Structure and stratigraphy of the south flank of the Kiseynew Domain in the Trans-Hudson Orogen, Manitoba: Implications for 1.845-1.77 Ga collision tectonics, *Can. J. Earth Sci.*, 36, 1859–1880, 1999.
- Zwanzig, H. V., E. C. Syme, and H. P. Gilbert, Updated trace element geochemistry of ca. 1.9 Ga metavolcanic rocks on the Paleoproterozoic Lynn Lake Belt, *Open File, Of99-13*, map, diskette, 48 pp., Manitoba Ind., Trade and Mines, Geol. Serv., Winnipeg, 1999.
- 
- G. Bienfait, C. Carbonne, C. Jaupart, and F. Rolandone, Institut de Physique du Globe de Paris, 4 Place Jussieu, 75252 Paris cedex 05, France. (cj@ccr.jussieu.fr; rolandon@ipgp.jussieu.fr)
- C. Gariépy, R. Lapointe, and J. C. Mareschal, GEOTOP, UQAM, C.P. 8888, Succ. Centre-Ville, Montréal, H3C 3P8, Canada. (jcm@volcan.geotop.uqam.ca)

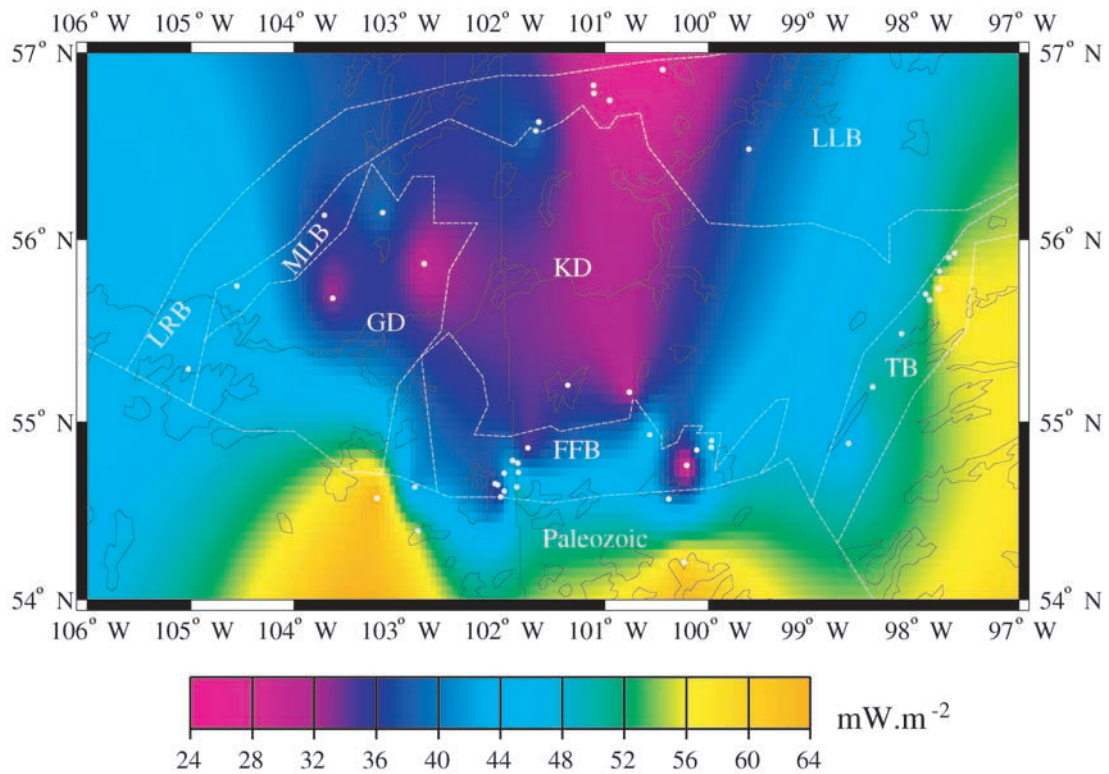


**Figure 8.** Heat flow map of the Trans-Hudson Orogen. White dots are the heat flow sites. The main belts of the Reindeer tectonic zone are outlined: Glennie Domain (GD), Flin Flon-Snow Lake Belt (FFB), Kiseynew Domain (KD), Lynn Lake Belt (LLB), La Ronge Belt (LRB), McLean Belt (MLB). The Thompson belt (TB) and the Paleozoic Cover are also indicated.